FINAL REPORT

"CONTINUOUS PROCESSING OF SOLID PROPELLANTS IN CO-ROTATING TWIN SCREW EXTRUDERS"

Grant No.: N00014-86-K-0620
BMDO/IST as managed by ONR

Highly Filled Materials Institute
Stevens Institute of Technology

REPORT DOCUMENTATION PAGE

Form Approved
OMB No. 0704-0188

1. AGENCY USE ONLY (Leave blank)	2. REPORT DATE	3. REPORT TYPE AND DATES COVERED
	October 5, 1995	Final Report (1986-1995)

4. TITLE AND SUBTITLE
"Continuous Processing of Solid Propellants in Co-Rotating Twin Screw Extruders"

5. FUNDING NUMBERS
N00014-86-K-0620

6. AUTHOR(S)
Prof. Dilhan M. Kalyon

7. PERFORMING ORGANIZATION NAME(S) AND ADDRESS(ES)
Stevens Institute of Technology
Highly Filled Materials Institute
Castle Point on the Hudson
Hoboken, NJ 07030

8. PERFORMING ORGANIZATION REPORT NUMBER

9. SPONSORING/MONITORING AGENCY NAME(S) AND ADDRESS(ES)
BMDO/IST as managed by ONR
Dr. Richard S. Miller, Project Manager
Mechanics & Energy Conversion S&T Division
Office of Naval Research - 800 N. Quincy St.
Arlington, VA 22217

10. SPONSORING/MONITORING AGENCY REPORT NUMBER

11. SUPPLEMENTARY NOTES

12a. DISTRIBUTION/AVAILABILITY STATEMENT
Applied for public release; distribution is unlimited.

12b. DISTRIBUTION CODE

13. ABSTRACT *(Maximum 200 words)*

The project developed mathematical models of twin screw extrusion processing of solid rocket fuels, which were validated using well-instrumented and industrial-scale twin screw extruders and processing simulants. The project further identified various safety concerns, ways of detecting and eliminating them and developed the techniques necessary to characterize the rheological behavior of highly-filled energetic materials. The findings of this project provide the science and technology base of the continuous processing of solid rocket fuels using co-rotating twin screw extruders.

14. SUBJECT TERMS			15. NUMBER OF PAGES
			16. PRICE CODE
17. SECURITY CLASSIFICATION OF REPORT	18. SECURITY CLASSIFICATION OF THIS PAGE	19. SECURITY CLASSIFICATION OF ABSTRACT	20. LIMITATION OF ABSTRACT
Unclassified	Unclassified	Unclassified	

DISCLAIMER NOTICE

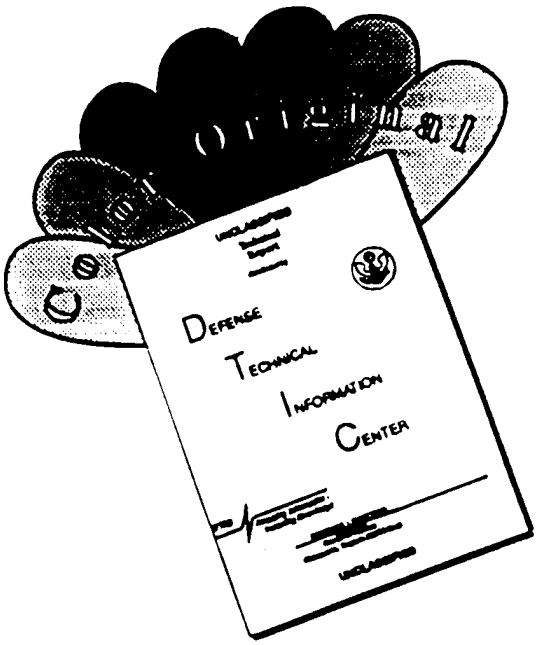

THIS DOCUMENT IS BEST QUALITY AVAILABLE. THE COPY FURNISHED TO DTIC CONTAINED A SIGNIFICANT NUMBER OF COLOR PAGES WHICH DO NOT REPRODUCE LEGIBLY ON BLACK AND WHITE MICROFICHE.

FINAL REPORT

"CONTINUOUS PROCESSING OF SOLID PROPELLANTS IN CO-ROTATING TWIN SCREW EXTRUDERS"

Grant No.: N00014-86-K-0620
BMDO/IST as managed by ONR

To: Dr. Richard S. Miller, Code 4435
Chief Scientist, Energy Conversion
Propulsion and Energetics Materials
Office of Naval Research
800 N. Quincy Street
Arlington, VA 22217

From: Prof. Dilhan M. Kalyon
Highly Filled Materials Institute
Stevens Institute of Technology
Castle Point on the Hudson
Hoboken, NJ 07030

Date: October 5, 1995

TABLE OF CONTENTS

I. Introduction

The objectives of our project funded by BMDO/IST as managed by ONR under the direction of Dr. Richard S. Miller were the following:

1. To develop a source code to mathematically model the thermo-mechanical history experienced by energetic materials during continuous processing in a co-rotating twin screw extruder.

2. To experimentally validate the mathematical model using well-instrumented industrial-scale twin screw extruders.

The project satisfied these objectives as well as discovering the following which have significant impact on the continuous processability of energetics.

- A particle-free region develops adjacent to all walls during the flow of energetic materials with their characteristic high degree of fill with solids.

- This particle free and binder-risk region at the wall gives rise to a region with a high -deformation rate and thus serves as an apparent slip layer.

- This thickness of this layer can be determined along with the wall slip velocity versus the imposed shear stress condition by using viscometric flows.

- The wall slip behavior needs to be incorporated into mathematical models of the process.

- The formation of this wall slip layer is affected by the presence of entrained air which further lubricates the surface.

- The binder polymer and the solids can separate along the flow direction where the basis of the demixing is the filtration of the binder in the flow direction. This filtration phenomenon is a well-defined safety hazard in processing of energetics.

- The amount of air entrained during processing is affected by screw geometrics and operating conditions used in extrusion.

• Extruders can develop hot spots. With increasing degree of fill of the energetic suspension, the relaxation time of the suspension increases (it becomes more solid-like) resulting in a yield stress (viscoplasticity), which exasparates the formation of the hot spot. The development of the hot spot is a safety hazard which should be eliminated.

• Twin screw extruders can convey energetic materials without mixing them giving rise to "pipeline" flows. The formation of such flow channels for unmixed materials constitutes a safety hazard and deteriorates the mixing efficiency of an extruder.

Our discovery of these phenomena specific to the highly filled nature of energetic materials lead us to develop tools (both experimental and theoretical) to elucidate them further. In the following, the understanding which we have gained from our studies of the flow and deformation, continuous processability, modeling and microstructure development aspects of processing of energetic suspensions are summarized. The publications which resulted from each area of study are also included and they can be consulted for further information. Finally, the processing configurations "lessons learned" from our studies are also included.

I.I. Issues

Manufacture of propellants, explosives and pyrotechniques (PEP´s) necessitate the processing of a energetic suspension or a dispersion at a solid concentration which approaches the maximum packing fraction, ϕ_m, of the solid phase. The concept of the maximum packing fraction is schematically illustrated in Figures 1-3. The use of a multimodal size distribution (Figure 2) is shown to increase the amount of solids which can be incorporated into a given volume i.e., a higher maximum packing fraction in comparison to a unimodal size (Figure 1), whereas the use of non-spherical and fibrous particles (Figure 3) decreases the maximum packing fraction [1].

The use of particles with different sizes is necessary in formulation of energetic materials to increase the maximum packing fraction. This is illustrated further in Figure 4. Here the maximum packing fraction is shown to be affected by the size

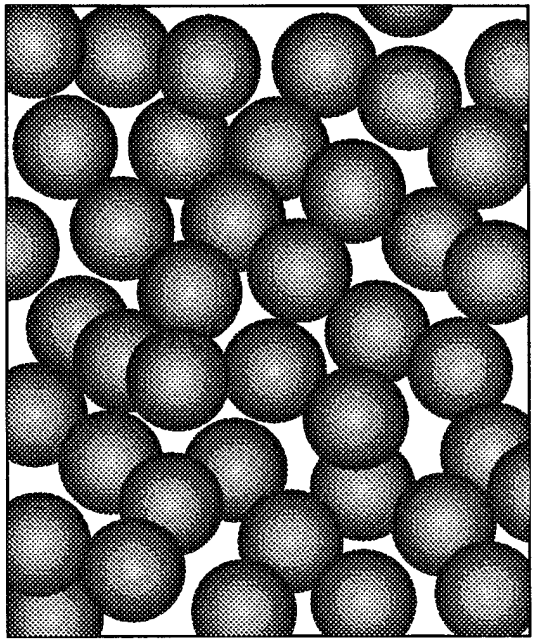

Figure 1. Packing of unimodal spherical particles and maximum packing fraction, i.e., maximum volume fraction, ϕ_m, of solids depending on the packing mode.
a) Simple cubic, $\phi_m = 0.52$
b) Body centered cubic, $\phi_m = 0.68$
c) Face centered cubic, $\phi_m = 0.74$

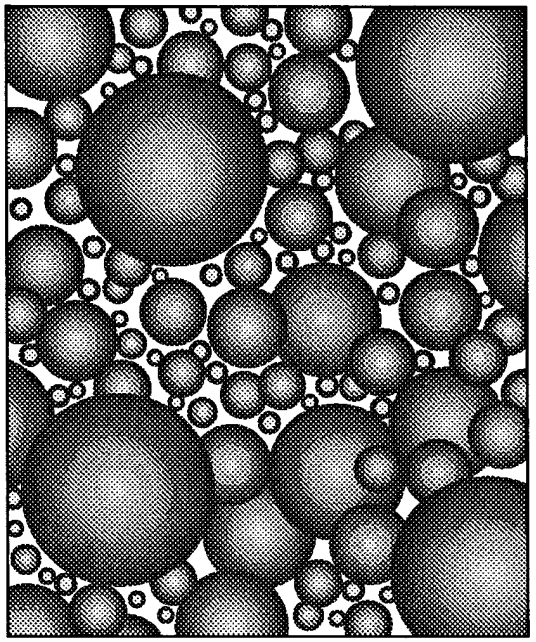

Figure 2. Packing of spherical particles with a multimodal particle size distribution $\phi_m = 0.90$.

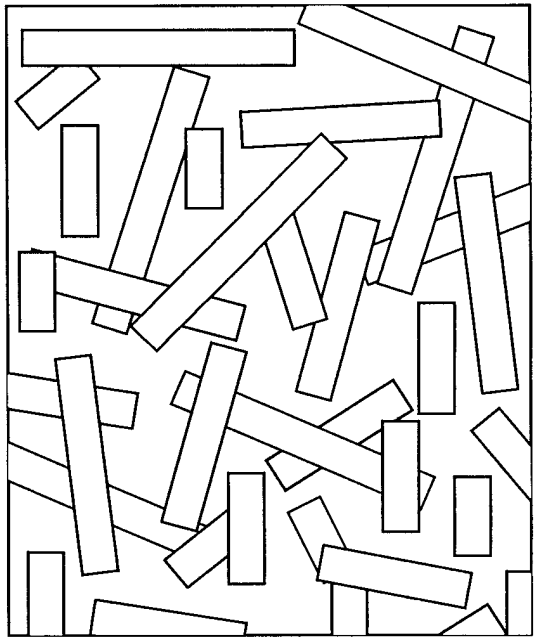

Figure 3. Packing of asymmetric particles with a low maximum packing fraction.

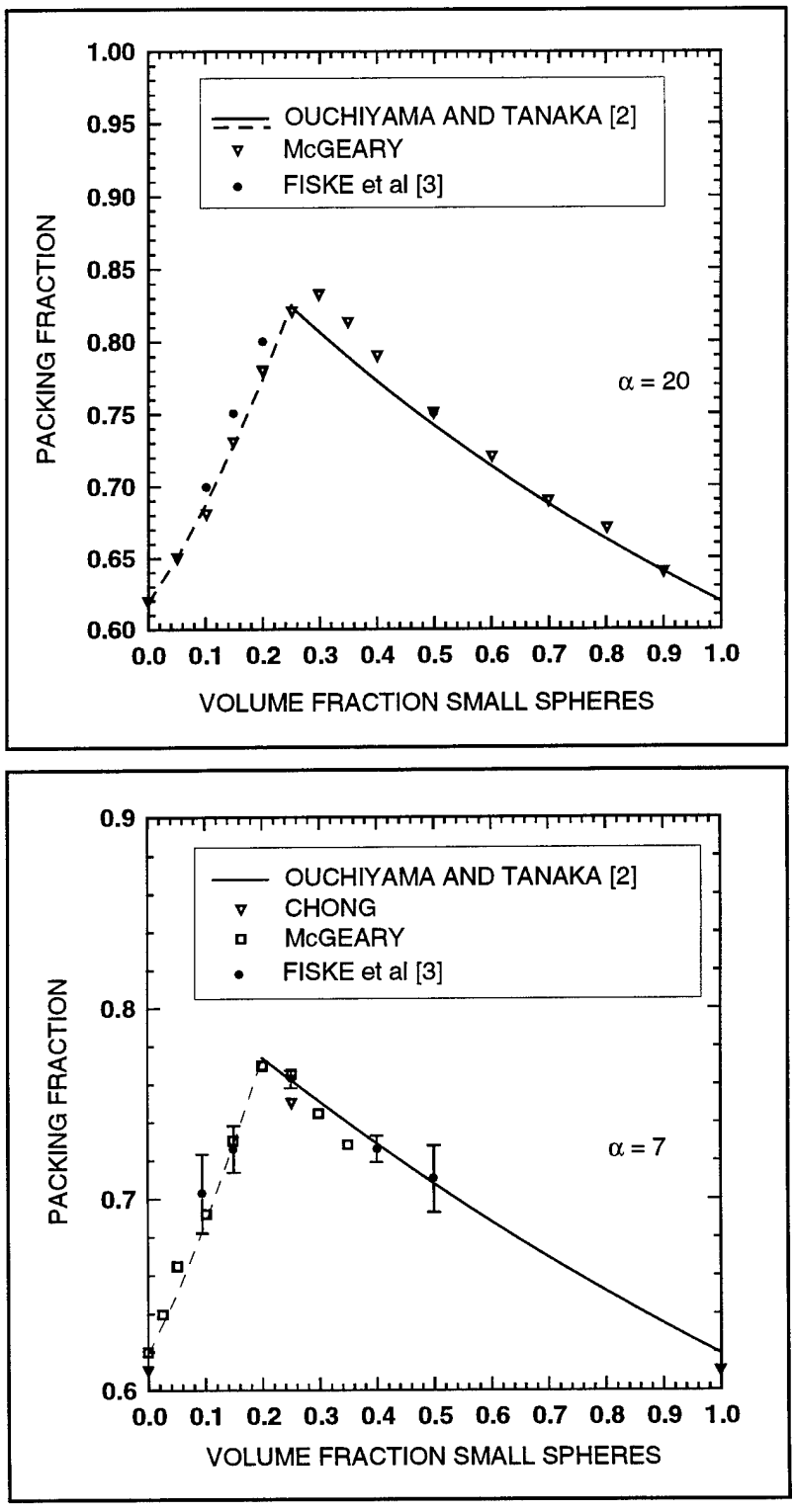

Figure 4. Maximum packing fraction versus size concentrations of spherical particles at different size ratios, α, for bimodal distribution: experiments and theory.

ratio, α, i.e., ratio of diameters of the large over small spheres, and the percentage of the smaller spheres in a bimodal particle size distribution [2, 3]. Thus, the shape and size distributions of solid particles are critical in determining the maximum possible concentration of solids incorporated into a suspension consisting of a liquid matrix phase (the binder) and solid particles.

The common denominator in propellant formulations is the use of the minimum amount of the liquid phase "binder" necessary to facilitate the flowability and shapeability of the energetic suspension and the maximum amount of solids to achieve the best-possible combustion properties. The minimal use of the binder by working close to the maximum packing fraction of the energetic solid phase reduces the porosity in the final grain. Overall, the high degree of fill of such highly concentrated energetic suspensions introduces significant difficulties in their characterization, processing, simulation, and quality control. However, propellants, regardless of their application, exhibit a number of common flow, deformation and processing traits which can be understood and used for their optimum design and operation of continuous manufacturing operations. In this final report, various hitherto identified traits will be outlined and ramifications on processing operations will be provided. The report will also review the simulation tools which we have developed.

As shown schematically in Figure 5, our research group has developed capabilities in simulation (using three dimensional Finite Element Method based source codes developed in house), rheological characterization, microstructural analysis, wettability and work of adhesion between solid and liquid phases, and characterization of ultimate properties of propellant formulations and their simulants. In the following, some of these experimental and numerical analysis tools will be described, along with some of the technologies developed.

III. **Flow and Deformation Behavior of Propellants and their Simulants**

The characterization of the flow and deformation behavior of propellants which are highly filled suspensions is first and foremost complicated by the occurrence of wall slip [4-16]. The wall slip behavior of a concentrated suspension consisting

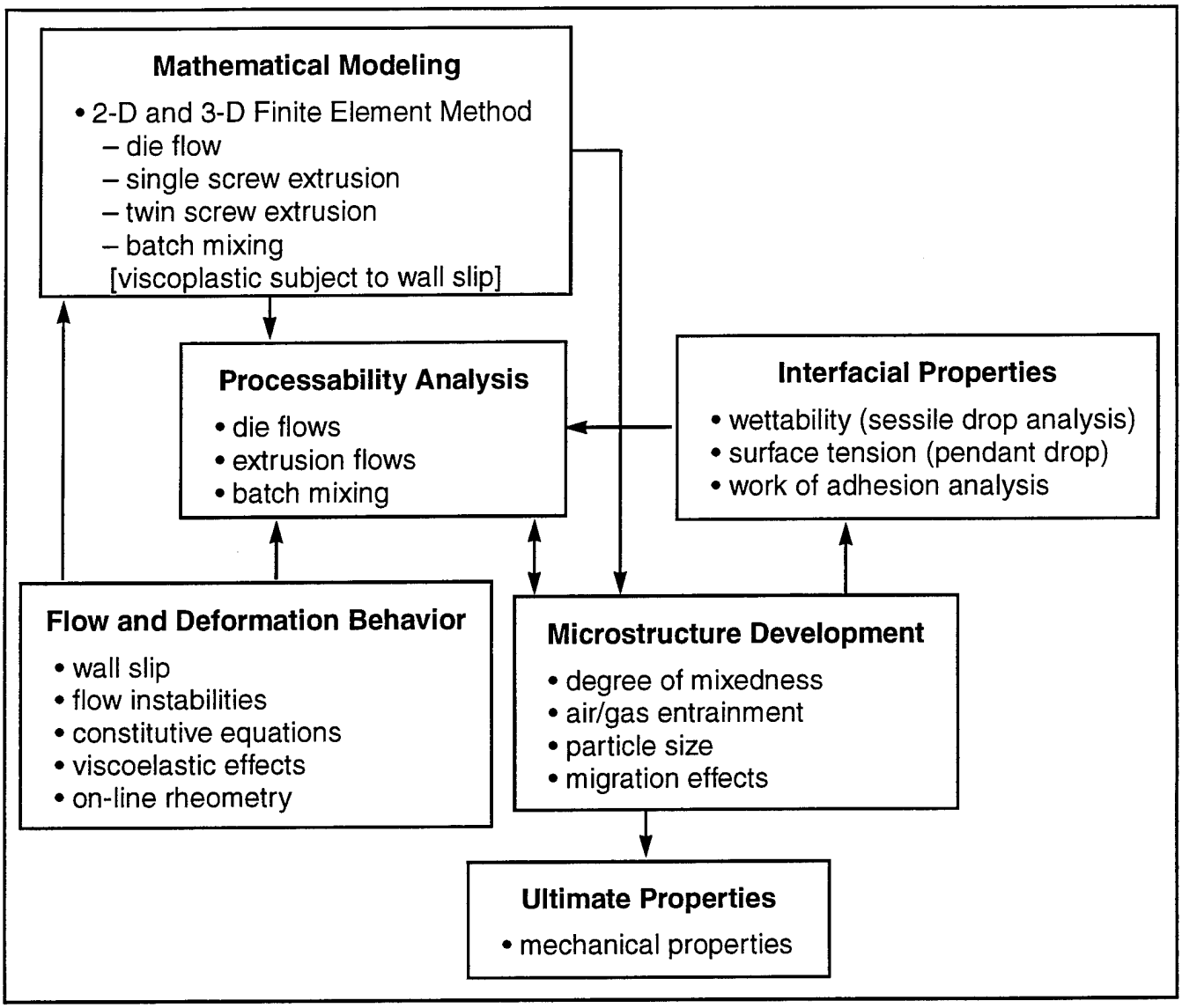

Figure 5. The integration of numerous capabilities developed.

of sixty three percent by volume of glass spheres in an acrylonitrile terminated polybutadiene, PBAN, matrix is demonstrated in Figure 6. The suspension sample undergoes steady torsional flow in between two parallel disks; the disk at the top is rotating and the disk at the bottom is stationary. Before the onset of deformation, a straight line marker is placed at the free surface of the suspension and the edges of the two disks. Upon the rotation of the top disk, discontinuities appear at both the top and bottom suspension/wall interfaces, indicating wall slip.

This technique which we have developed allows the unambiguous determination of the slip velocity and the true deformation rate of the suspension directly [13]. Computerized image analysis of the recorded images generates the velocity of the suspension found adjacent to the wall, $\vec{V}_f$ as a function of time. The slip velocity at the wall, $\vec{U}_s$, is $\vec{U}_s = \vec{V}_f - \vec{V}_w$, where $\vec{V}_w$ is the wall velocity. This is one of the techniques we have used to characterize the wall slip behavior of propellants and their simulants.

In Figure 7 the time dependent development of the wall slip behavior of a suspension in steady torsional flow is shown [16]. With time, the deformation rate of the suspension decreases, while the shear stress and the wall slip velocity increase. When the steady state behavior is achieved, the true deformation rate is only about 1/5th of the imposed apparent shear rate. The thickness of the slip layer can be estimated as a function of the viscosity of pure polymer binder and is generally in the order of microns [9, 13, 16].

If the surface to volume ratio in rheometry is systematically changed, the slip velocity can be determined also from the slope of the apparent shear rate versus reciprocal diameter or gap data collected at constant wall shear stress. For example, in steady parallel disk torsional flows the apparent shear rate at the edge, $\dot{\gamma}_{aR}$, becomes proportional to reciprocal of the gap between the two disks, I/H [7]. Plots of apparent shear rate, $\dot{\gamma}_{aR}$, versus the reciprocal gap height, 1/H, at constant values of shear stress, τ_R, generate straight lines with slopes equal to 2 $U_S(\tau_R)$ as shown in Figure 8 [8, 9, 13, 14]. The slope hence the slip velocity values increase with increasing wall shear stress. On the other hand, in capillary flow changing the surface to volume ratio requires that the capillary diameter be changed while keeping the length/diameter ratio of the capillary a constant. Upon wall slip, the apparent shear rate varies linearly with reciprocal of capillary

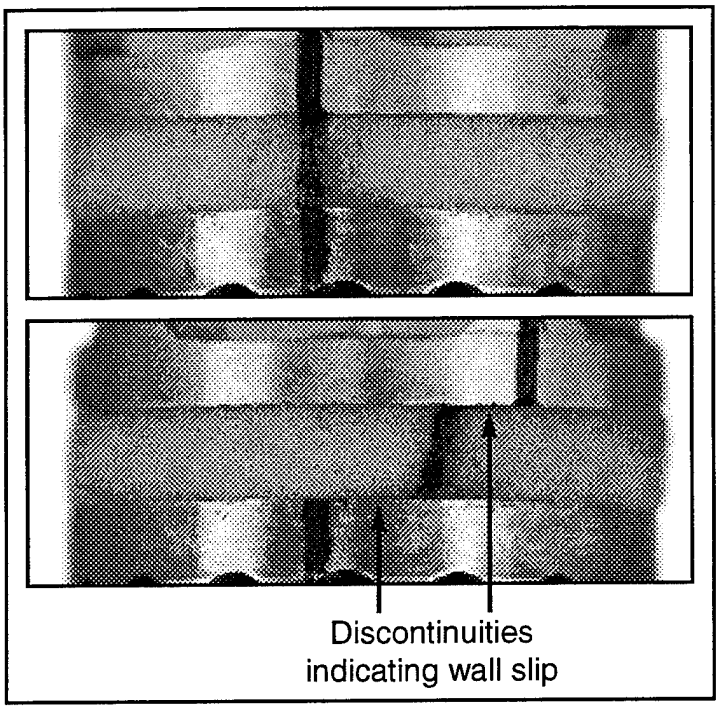

Figure 6. Demonstration of wall slip of a concentrated suspension in steady torsional between two parallel disks.

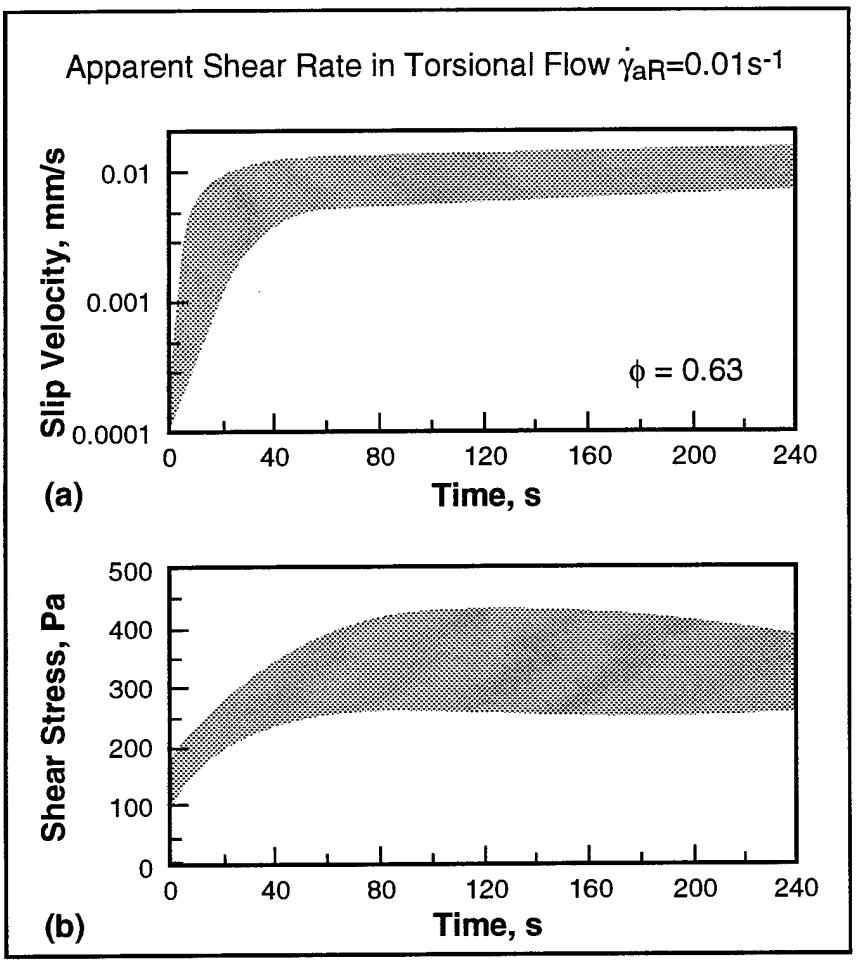

Figure 7. Time-dependent development of wall slip in torsional flow of a PBAN suspension with 63% by volume spherical solids.

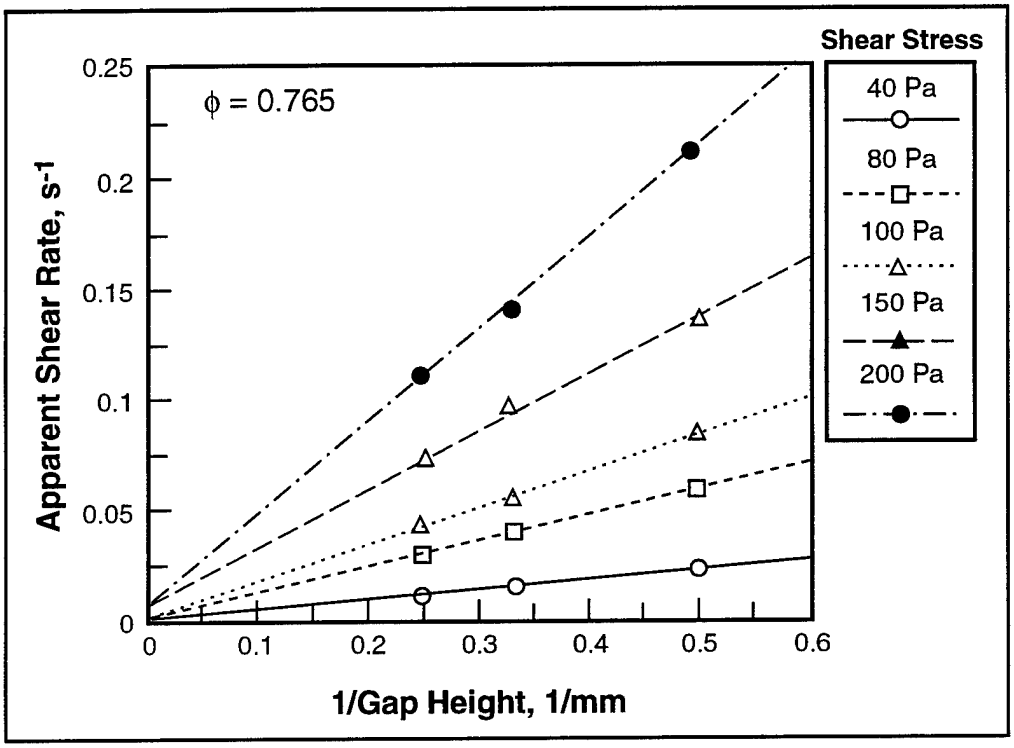

Figure 8. Apparent shear rate versus reciprocal of gap height for a suspension with 76.5% by volume solids in steady torsional flow.

diameter, 1/D, at constant wall shear stress with a slope equal to $8U_S$ [4, 9], where U_S is the wall slip velocity. The typical steady-state slip velocity at the wall versus wall shear rate behavior of two propellant simulants are shown in Figure 9. The wall slip velocity, U_S, varies linearly with wall shear stress, τ_R [9, 13].

IV. Solid-like Behavior with Wall Slip

The relative effect of the slip flow on the overall flow rate in a die with an equivalent diamter of D, can be ascertained by the characterization of the Q_S/Q ratio where Q_S is the volumetric flow rate due to slip i.e., $Q_S = (\pi/4)D^2U_S$ and Q is the volumetric flow rate given by $Q = (\pi/4)D^2V$. When the mean velocity of the suspension in the die, V, becomes equal to the slip velocity, U_S, the suspension flows without deformation, that is as a plug, lubricated at the wall.

Q_S/Q versus wall shear stress behavior of two propellant simulants in capillary flow are shown in Figure 10. The data indicates that the 60 percent by vol. solids propellant simulant flows as a plug above a wall shear stress value of 40 kPa, whereas the suspension with 76.5 percent by vol. solids exhibits plug flow in the capillary, at wall shear stress values which are smaller than about 10 kPa [9, 13].

These observations indicate that propellants become solid-like in various flow regimes. Solid-like behavior at wall shear stress values smaller than a yield stress is defined as viscoplasticity and is related to the formation of a temporary network which is destroyed when the shearing stress exceeds the yield stress. On the other hand, we have found that the development of solid-like behavior above a critical wall shear stress is associated with dilatancy [17] possibly arising from the radial migration of solid particles away from the wall of the die [18-20] and/or interlocking to establish solid-like behavior.

Figure 11 illustrates the viscoplasticity of a propellant simulant with 76.5% by volume solids [13]. This is the simulant which was used to develop the process in the Advanced Shuttle Rocket Motor Project run by Lockheed/Aerojet consortium. Upon rotation of the disk at the top, the propellant simulant initially deforms. However, further angular displacement of the rotating disk induces only wall slip adjacent to the walls and the propellant simulant no longer deforms under the prevailing conditions of constant shear stress. The inseparable nature

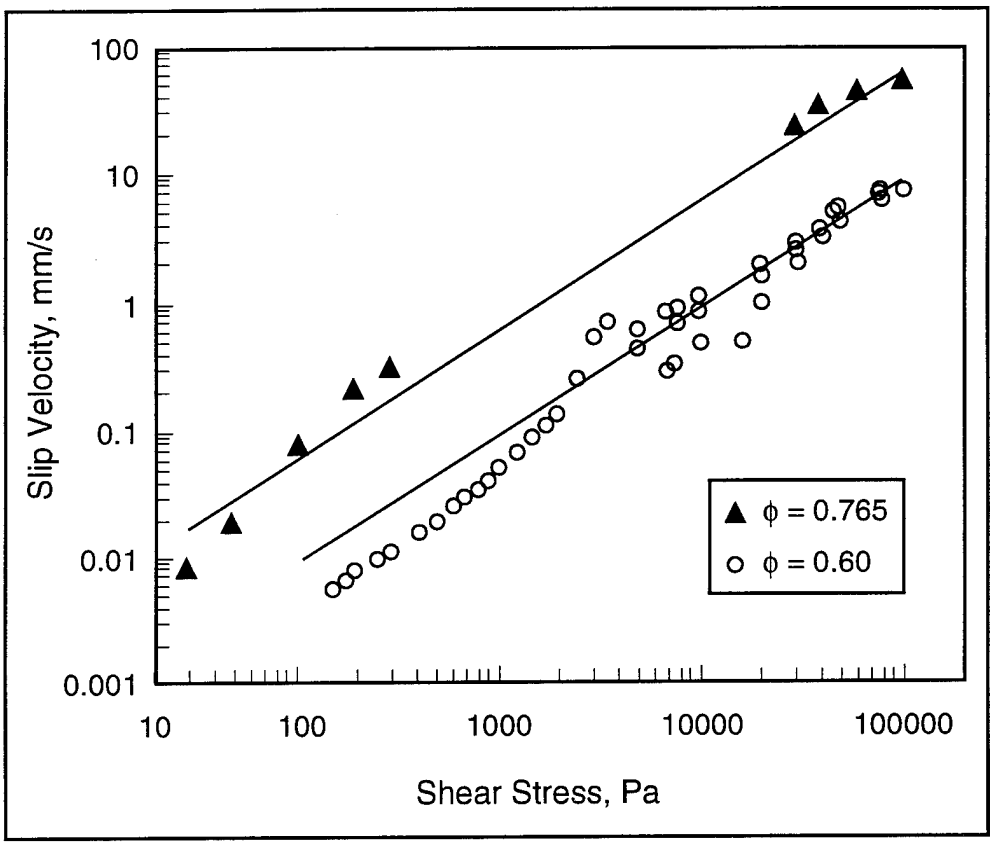

Figure 9. Wall slip velocity versus shear stress of two suspensions with 60% and 76.5% by volume solids.

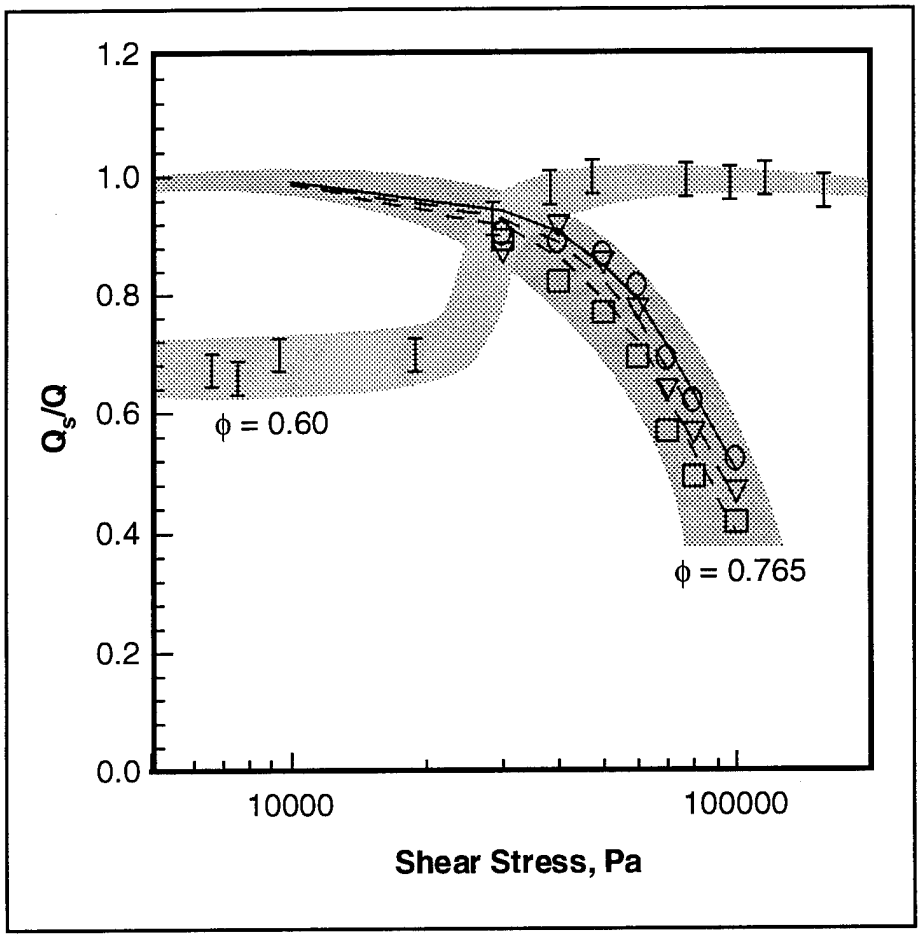

Figure 10. Ratio of volumetric flow rate due to slip, Q_s over volumetric flow rate for capillary flow, Q, of two suspensions with 60% and 76.5% by volume solids.

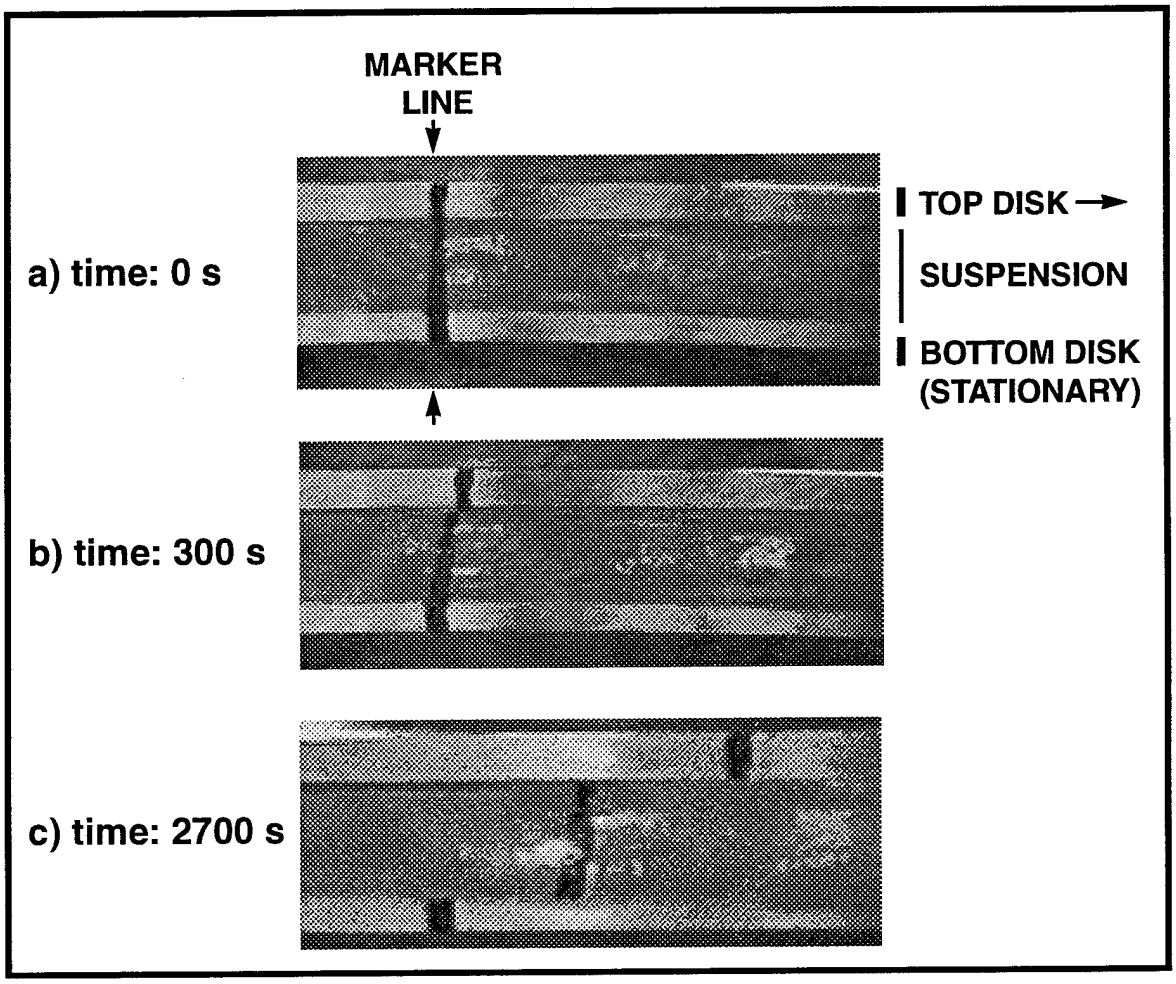

Figure 11. Demonstration of the viscoplasticity, i.e., solid-like behavior at a shear stress smaller than yield stress.

of wall slip and solid-like behavior of propellants and their simulants is thus emphasized.

V. Flow Instabilities of Propellants and their Simulants

We have discovered that the pressure driven flows of propellants can give rise to flow instabilities associated with the migration of the polymeric binder in the direction of the pressure gradient, which drives the flow [21-24]. Such demixing of the ingredients of the formulation of highly filled suspensions affects the quality of the degree of mixedness of the suspension and hence its ultimate properties. It renders the continuous processing operation unstable and also poses a safety threat in processing of energetic suspensions. The use of gear pumps or sensors with tight converging sections also become prohibiting for propellants and other PEP's.

The basic driving force of flow instabilities in the flow of propellants is the axial migration of the binder, "filtering," superimposed on the pressure-induced bulk flow of the energetic suspension. Upon axial migration concentration gradients develop in the energetic suspension found in the reservoir under pressure and the extrudate emerging from the die. The axial migration of the binder phenomenon is demonstrated in Figure 12 [24]. Here, upon the pressure induced flow of a suspension in a cylindrical reservoir connected to a capillary die, the propellant simulant suspension (used in ASRM program for solid rocket motors) loses some of its binder content and develops a concentration gradient in the axial flow direction, z, between the plunger which drives the flow and the die. Under severe unstable flow conditions the pressure necessary to extrude the propellant oscillates while growing unbounded with time. The time periodic oscillations in extrusion pressure are related to the time periodic mechanism of formation of a mat of solids at the capillary or die and its break-up which occurs concomitant with the filtration of the binder in the axial direction [22].

The onset of flow instabilities associated with mat formation and filtering of the binder can be predicted with reasonable accuracy by comparing the filtration velocity, V_m (average velocity of the binder through a packed bed of solids) of the binder with the wall slip velocity, U_s, under the generally prevailing plug flow conditions [22,24]. The flow generally becomes unstable when the filtration

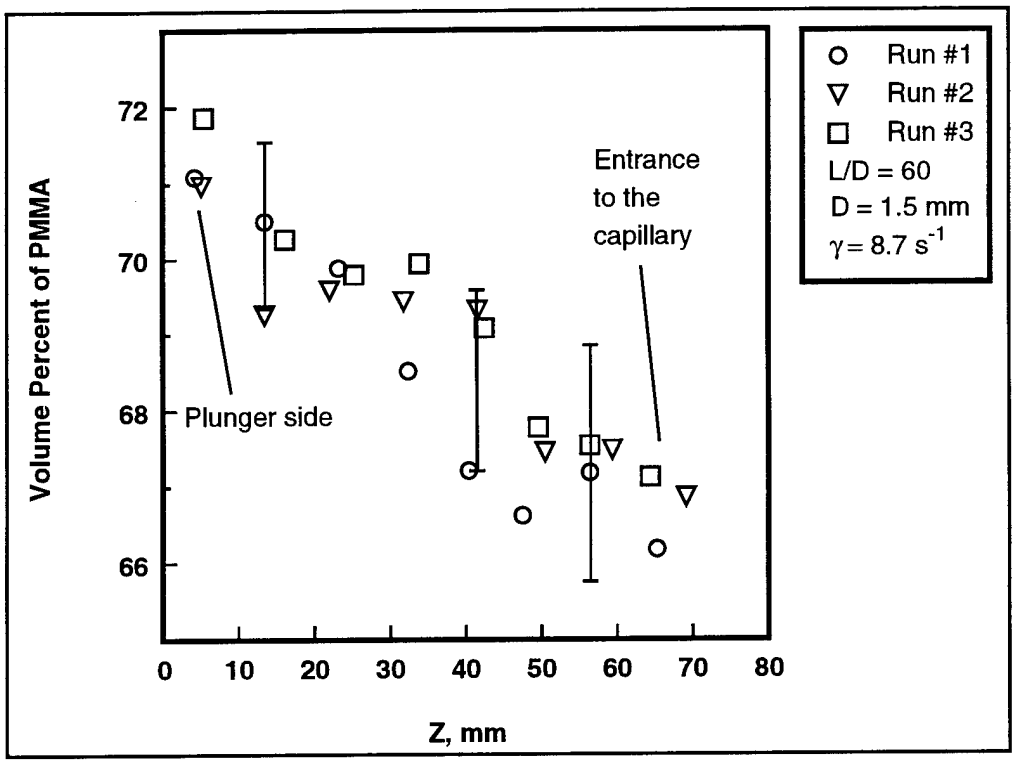

Figure 12. Concentration gradient development in a density matched suspension (64.6% solid polymethyl methacrylate particles in polyether oil based binder) upon pressure flow in a cylindrical reservoir connected to a capillary die [24].

velocity V_m of the binder becomes greater than the slip velocity of the propellant plug. This phenomenon is shown in Figure 13 for the ASRM propellant simulant containing 76.5 percent vol. solids. Line C-C´ represents the points where the slip velocity, U_s, is equal to the filtration velocity of the binder. Theoretically, extrusion at apparent shear rates found to the left of line C-C´ is subject to the time-periodic filtering of the binder and constitute the unstable region. The range compares favorably with the experimentally observed thresholds for the on-set of flow instabilities represented by line B-B'.

Obviously in the processing of propellants the filtration of the matrix and thus the unstable region should be avoided [21-24]. Otherwise, the additional loss of the binder due to axial migration of the polymeric binder at solid loading levels, which are very close to the maximum packing fraction of the fuel and oxidizer particles will render the propellant unprocessable. The unstable region in converging flows can be avoided by the proper selection of the production rate and the geometry of the channel through which the suspension is flowing. We have studied some of the pertinent factors and reported on their effects to help the propellant industry to properly select their geometries and operating conditions (14, 21-24).

VI. Air Entrainment Effects in Processing of Propellant Suspensions

Since the formulation of a highly filled propellant suspension involves a volume fraction of solids i.e., fuel and oxidizer particles which approaches the maximum packing fraction of the solid phase, the incorporation of even small concentrations of air, makes a significant difference in the rheological behavior and hence the processability of propellant filled suspensions [25-29]. The shear viscosity of the energetic suspension decreases and wall slip velocity values increase with the incorporation of air into the propellant [28].

The amount of air entrained into the energetic suspension increases at partially full regions in comparison to suspension samples found at the completely full sections of processors during the continuous processing of propellants and their simulants [26]. The density of samples collected from the reversely configured screw sections of a twin screw extruder (which necessitate completely full mixing volume) are greater than those of the samples collected from the partially full

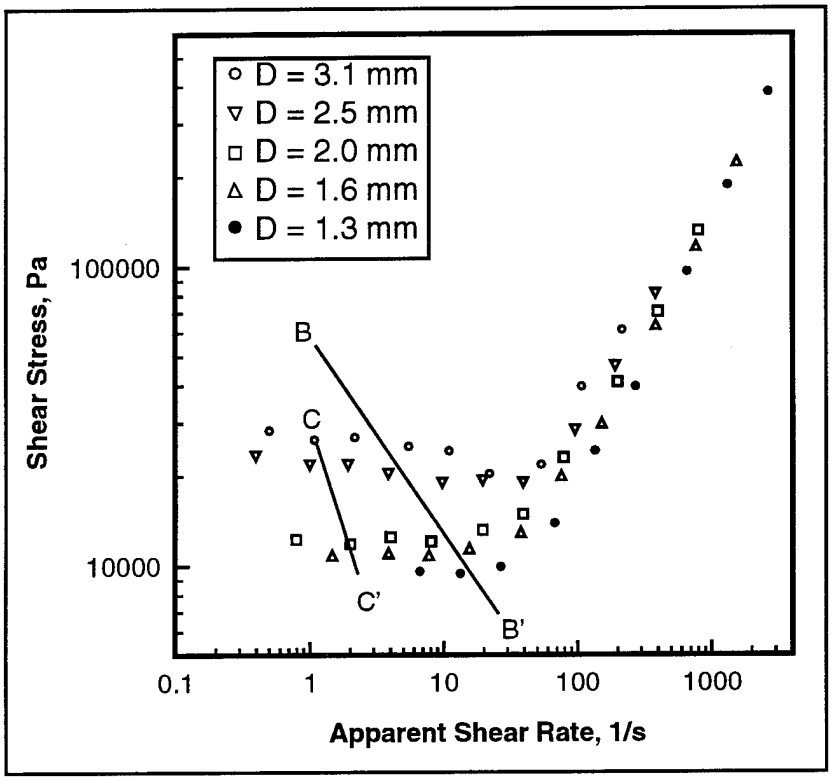

Figure 13. Experimentally (B-B') and theoretically (C-C') determined unstable flow zone in capillary flow of a suspension with 76.5% solids [24].

sections of the same extruder i.e., at forwardly configured screw sections [26]. The air entrained into the suspension also affects the development of the slip layer (binder rich region found adjacent to the wall) of the suspension during die flows [30]. Under moderate die pressures, pockets of air cling to the wall momentarily and are spread out to be later dragged-on by the bulk of the suspension [30].

VII. Mathematical Modeling of Twin Screw Extrusion of Propellants

Currently twin screw extrusion processing is used in various processing applications where the ingredients of a propellant formulation are interpersed in each other (distributive mixing), the physical properties of one or more of the components are altered (dispersive mixing such as a decrease in particle size), the air or solvent content of the suspension is reduced under vacuum (devolatilization), and the energetic suspension is pressurized (for shaping in a die or mold); all within the confines of a single processor with properly selected screw and barrel elements [31]. Such versatile continuous processors provide a better surface to volume ratio and facilitate real-time, on-line process control and easier pollution prevention in comparison to batch mixers. However, due to the peculiar nature of the flow and deformation behavior of propellants with very high degree of fill their twin screw extrusion processing modeling is a special challenge [32-41]. For example, the wall slip behavior needs to be incorporated into the mathematical modeling of their processing behavior [32, 33, 35, 38, 39]. Figure 14 shows the typical effect of the ratio of the wall slip coefficient at the screw surface over the slip coefficient at the barrel surface, φ, on the operating curve of a single screw extruder [32]. At constant mass flow rate the pressurization capability decreases with increasing slip coefficient ratio, φ.

Simulation Techniques Developed

Flow Equations

The governing equations of the flow in the extrusion flow are given by the general equations of conservation of mass and momentum, which are fully elliptic and three-dimensional. For regular flighted elements simplifying assumptions can be made which render the equations parabolic and, therefore, amenable to

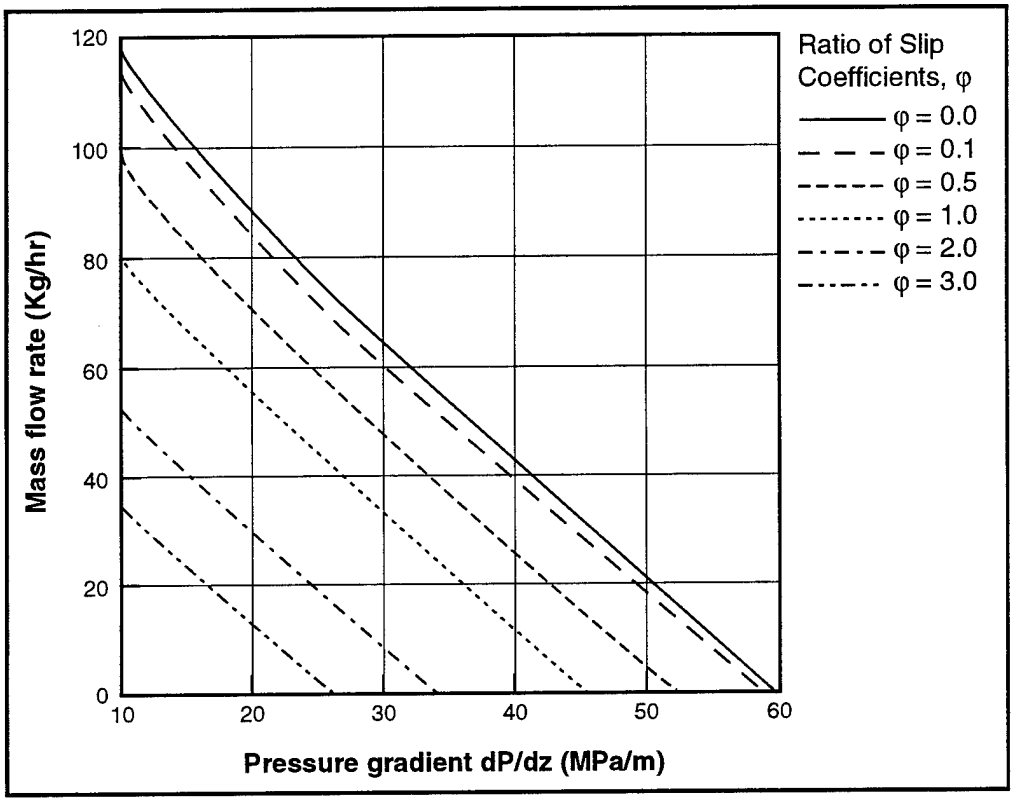

Figure 14. Operating curve (pressurization rate versus production rate) of a single screw extruder as affected by the ratio of wall slip coefficients at screw and barrel surfaces, φ [32].

stepwise integration in the z-direction (primary flow direction) from prescribed upstream conditions. These assumptions are as follows:

(i) the inertia effect is negligible because of the highly viscous nature of the generally polymeric materials used in extrusion and the creeping nature of the resulting flow,
(ii) the flow is steady,
(iii) the screw channel can be unwound in a helical direction of the screw,
(iv) the velocity derivatives along the channel are small compared to those in the transverse directions except for locations that are close to the entrance, and
(v) the barrel moves relative to the screw at an angle (i.e. the helix angle) to the downchannel direction with a constant velocity given by the screw rotational speed and barrel diameter.

However, for kneading disc type elements the flow field can only be solved in 3-D.

The equations of conservation of mass and momentum are:

$$\frac{\partial u_x}{\partial x} + \frac{\partial u_y}{\partial y} + \frac{\partial u_z}{\partial z} = 0 \qquad (1)$$

$$\frac{\partial \overline{p}}{\partial x} = \frac{\partial}{\partial x}\left(2\eta \frac{\partial u_x}{\partial x}\right) + \frac{\partial}{\partial y}\left\{\eta\left(\frac{\partial u_x}{\partial y} + \frac{\partial u_y}{\partial x}\right)\right\} \qquad (2)$$

$$\frac{\partial \overline{p}}{\partial y} = \frac{\partial}{\partial y}\left(2\eta \frac{\partial u_y}{\partial y}\right) + \frac{\partial}{\partial x}\left\{\eta\left(\frac{\partial u_x}{\partial y} + \frac{\partial u_y}{\partial x}\right)\right\} \qquad (3a)$$

$$\frac{dp_m}{dz} = \frac{\partial}{\partial x}\left(\eta \frac{\partial u_z}{\partial x}\right) + \frac{\partial}{\partial y}\left(\eta \frac{\partial u_z}{\partial y}\right) \qquad (3b)$$

where the asterisk (*) denoting the dimensionless forms of the variables has been suppressed in the equations for convenience. For regular flighted screw

sections the parabolic nature of these differential equations is preserved through p_m, the mean viscous pressure which has been defined for the primary flow direction, z, and is constant for any x-y plane. The pressure gradient in the downchannel direction pressure gradient, dp_m/dz, which is a function of the channel direction coordinate, z, for temperature dependent shear viscosity, is determined by the requirement that the conservation of mass constraint on the total volumetric flow rate is satisfied, i.e.:

$$Q - \int_D u_z dD = 0 \tag{4}$$

where Q is set by the specified inlet value of dp_m/dz. The pressure $\overline{p}$, is allowed to vary in the transverse directions in such a way that the continuity equation (Eq. 1) is satisfied. For regular flighted elements, even though u_z varies along the downchannel direction, z, it may be assumed in Eq. (1) that step sizes in z direction are so small that $\partial u_z/\partial z$ is negligible compared to the other two terms. Equations (2a) and (2b) can now be handled separately from the channel direction equation (2c), and the penalty method is used in approximating the pressure $\overline{p}$.

Boundary Conditions and Implementation of Wall Slip

Applying Bubnov-Galerkin's method to Eqs.(2a) and (2b) leads to the following dimensionless residual equations:

$$\int_D \nabla\pi \cdot \underline{\underline{T}} dD - \int_{\Gamma_s} \pi(\mathbf{n} \cdot \underline{\underline{T}})\, d\Gamma_s = \mathbf{0} \tag{5}$$

where π is the weighting function and $\underline{\underline{T}}$, the total stress tensor is as modified by the parabolic flow assumption. On the boundaries, the traction $\mathbf{n} \cdot \underline{\underline{T}}$ can be decomposed into the tangential and normal components to obtain:

$$\int_D \nabla\pi \cdot \underline{\underline{T}}\, dD - \int_{\Gamma_s} \pi(\mathbf{nt} : \underline{\underline{T}})\mathbf{t}\, d\Gamma_s - \int_{\Gamma_s} \pi(\mathbf{nn} : \underline{\underline{T}})\mathbf{n}\, d\Gamma_s = \mathbf{0} \tag{6}$$

where **t** and **n** are respectively the unit tangent and the unit outward normal vectors to the solid boundary. Eqs. (2a) and (2b) are required to be satisfied on the boundary. The conditions of wall slip and no material exchange between the fluid and the boundary in dimensionless form can be expressed as:

$$\mathbf{t} \cdot (\mathbf{u} - \mathbf{u}_{solid}) = \beta^* (\mathbf{nt} : \underline{\underline{\mathbf{T}}}) \tag{7a}$$

$$\mathbf{n} \cdot (\mathbf{u} - \mathbf{u}_{solid}) = 0 \tag{7b}$$

where $\mathbf{u}_s$ is the solid boundary velocity, $\mathbf{u}$ is the fluid velocity, $\beta^* = (m_o \omega^{n-1} / R_s)\beta$ is the dimensionless Navier's slip coefficient, i.e., $\beta = 0$ gives no slip and $\beta = \infty$ is perfect slip. Eq. 7a is the Navier's slip condition as applicable to the two-dimensional transverse plane [23].

Referring now to Eq. 6 for the implementation of the boundary conditions, one observes that while the slip condition easily blends with it by providing the tangential component of the traction, the normal component presents a difficulty as it is not recoverable from the second condition, i.e., Eq. 7b, which gives only the normal velocity. In essence, the numerical difficulty posed by a slip boundary condition is the requirement that both the essential (kinematic) condition (Eq. 7b) and the natural (Navier's slip) condition be satisfied at every boundary nodes. We have transformed the essential condition of normal velocity into a natural condition [25]:

$$\mathbf{nt} : \underline{\underline{\mathbf{T}}} = \frac{\mathbf{t} \cdot (\mathbf{u} - \mathbf{u}_{solid})}{\beta^*} \tag{8a}$$

$$\mathbf{nn} : \underline{\underline{\mathbf{T}}} = \frac{\mathbf{n} \cdot (\mathbf{u} - \mathbf{u}_{solid})}{\lambda_s} \tag{8b}$$

where a new penalty parameter, λ_s, has been introduced. As $\lambda_s \rightarrow 0$, Eq. 8b becomes equivalent to Eq. 7b since the normal component of the traction must be finite at the boundary. In practice, a λ_s value in the range 10^{-10} - 10^{-18} produces a normal velocity difference of the same order of magnitude. Equations 8a-b are now substituted into Eq. 6 to give:

$$\int_D \nabla\pi \cdot \underline{\underline{\mathbf{T}}}\, dD - \int_{\Gamma_S} \pi \frac{\mathbf{t}\cdot(\mathbf{u}-\mathbf{u}_{solid})}{\beta^*}\, \mathbf{t}\, d\Gamma_S - \int_{\Gamma_S} \pi \frac{\mathbf{n}\cdot(\mathbf{u}-\mathbf{u}_{solid})}{\lambda_S}\, \mathbf{n}\, d\Gamma_S = \mathbf{0} \qquad (9)$$

This method is generally applicable to any rheological behavior, geometrical shape of the boundary, and orientation. For the channel direction momentum equation, the normal component of traction does not exist–which makes the incorporation of wall slip by the Galerkin method straightforward. The components of $\mathbf{u}_{solid}$ on the screw root surface are all zero while on the barrel, the solid boundary velocity $\mathbf{u}_{solid}$, is given in dimensionless form as:

$$\mathbf{u}_{solid} = \mathbf{i}\sin\phi + \mathbf{k}\cos\phi \qquad (10)$$

where ø is the helix angle of the screw and, **i** and **k** are unit vectors in x- and z-directions respectively.

Constitutive Model

The propellant formulations are assumed to be purely viscous fluids which can be characterized rheologically by the generalized Newtonian fluid constitutive relation:

$$\underline{\underline{\mathbf{T}}} = -\eta(\dot{\gamma})\,\underline{\underline{\dot{\gamma}}} \qquad (11)$$

where η is the shear viscosity material function, $\underline{\underline{\dot{\gamma}}}$ is the rate-of-deformation tensor and $\dot{\gamma}$ is the deformation rate. The dependence of the shear viscosity material function on the deformation rate and temperature follows the modified Herschel-Bulkley model:

$$\eta = \left[m_o|\dot{\gamma}|^{n-1} + \frac{\tau_y(1-\exp(-n_b|\dot{\gamma}|))}{|\dot{\gamma}|} \right] \exp(-c'(T-T_o)) \qquad (12)$$

where n is a material parameter which governs the sensitivity of the fluid to deformation rate, τ_y is the apparent yield stress, n_b is the stress growth exponent, c´is the temperature coefficient of viscosity, with T_o, the entrance

temperature as the reference temperature. The magnitude of the rate-of-deformation tensor $|\dot{\gamma}|$ is defined for our case, by:

$$|\dot{\gamma}|^2 = 2u_{x,x}^2 + 2u_{y,y}^2 + (u_{x,y} + u_{y,x})^2 + u_{z,x}^2 + u_{z,y}^2 \qquad (13)$$

where comma indicates differentiation. If we introduce the following dimensionless variables:

$$|\dot{\gamma}| = \omega|\dot{\gamma}|^*, \tau_y = m_o\omega^n\tau_y^*, n_b = n_b^*/\omega \qquad (14)$$

then Eq. 12, in dimensionless form, becomes:

$$\eta^* = \left[(|\dot{\gamma}|^*)^{n-1} + \frac{\tau_y^*(1-\exp(-n_b^*|\dot{\gamma}|^*))}{|\dot{\gamma}|^*}\right]\exp(-c'(T-T_o)) \qquad (15)$$

Various simplifications of the modified Herschel-Bulkley model include the Ostwald-de Waele power-law fluid ($\tau_y^* = 0$), the Newtonian fluid (n=1, $\tau_y^* = 0$), the modified Bingham plastic (Papanastasiou [26], (n=1) and the classical Bingham plastic fluid above the yield point (n=1, $n_b^* = \infty$). For any given propellant formulation the parameters of the constitutive equation need to be determined using the viscometric flows discussed earlier. The Navier's wall slip coefficient β^* also needs to be characterized for a given propellant from viscometric experimental techniques which we have developed (8, 9, 12, 13, 16).

Energy Equation and Boundary Conditions

By an order-of-magnitude analysis of the energy equation, it can be demonstrated that in the extrusion flow the importance of the transverse convection terms ($\rho C_p u_x \partial T/\partial x$, $\rho C_p u_y \partial T/\partial y$) relative to heat conduction in y-direction scales as $Pe\, u_x^* H^2/W$ where $Pe = \rho C_p \omega R_s^2/k$ is the Peclet number and H and W are respectively, the dimensionless maximum depth and width of the screw channel. Polymeric binders and propellants generally have low thermal conductivity and, moderately high values of ρ and C_p, hence exhibit high Peclet number. Therefore, the transverse convection term will be negligible only for

small H and large W (i.e. low aspect ratio geometries) and also for small helix angle. If the transverse convection term is compared with the downchannel convection term, the transverse convection term will be negligible if the ratio $u_x^* z^* / u_z^* W$ is small, where u_x^* and u_z^* are dimensionless. For the regular flighted element, from the continuity equation and the typical choice of the step size, u_z^* / z^* is generally small. Hence, the transverse convection terms can be ignored only if W is very large or the helix angle is very small—the same conditions as obtained earlier. Since these conditions are rarely encountered in the design and operation of realistic extruders, the transverse convection terms should be included in the energy equation for the analysis of extrusion flows.

By a similar analysis, the quantity $Pe u_z^* z^*$ governs the relative importance of the downchannel convection to heat conduction in the downchannel direction. Therefore, except for low volume flow rates and the region very close to the entrance, one can neglect heat conduction in the downchannel direction since the Peclet number is generally high. With these assumptions and the assumption of steady state conditions, using the dimensionless temperature $\theta = (T - T_o) / (T_b - T_o)$, the energy equation in dimensionless form becomes:

$$Pe\left(u_x \frac{\partial \theta}{\partial x} + u_y \frac{\partial \theta}{\partial y} + u_z \frac{\partial \theta}{\partial z}\right) = \left(\frac{\partial^2 \theta}{\partial x^2} + \frac{\partial^2 \theta}{\partial y^2}\right) + G\eta^*\left(|\dot{\gamma}|^*\right)^2 \qquad (16)$$

where $G = m_o \omega^{n-1} (\omega R_s)^2 / k(T_b - T_o)$ is the Griffith number (generally referred to as the Brinkman number for the Newtonian fluid). The asterisk (*) denoting the dimensionless forms has been suppressed for the velocity components and co-ordinates. The Griffith number indicates the relative importance of viscous dissipation effects to heat conduction.

The fluid enters the screw channel at a temperature T_o. The barrel temperature is designated as T_b and is different from the entrance temperature. Variations in T_b along the channel direction are allowed. Although our model can be used in conjunction with any type of thermal boundary condition, we have found that constant barrel temperature and adiabatic screw surface conditions are proper boundary conditions. Thus, in dimensionless form, the initial and boundary conditions become:

at $z = 0$, $\theta = 0$
on barrel surface $\theta = 1$
on screw surface $\partial\theta / \partial \mathbf{n} = \mathbf{0}$ (17a-c)

where **n** is the unit vector normal to screw surface. Equation (16) was initially solved with the above specified boundary conditions using the Bubnov-Galerkin method and the removal of oscillations in the temperature solution was initially attempted by a simple smoothening procedure. However, later we modified our algorithms to implement the recently developed SUPG method (which has rarely been implemented in polymer extrusion simulation) by introducing weighting functions of the form:

$$\overline{W}^f = W^f + w^f \tag{18}$$

where W^f is a continuous function of space and w^f is a discontinuous perturbation of W^f. The weighted residual form of the energy equation is then given by:

$$\int_z^{z+\Delta z} \left\{ \int_D \left[\overline{w}^f Pe \left(u_x \frac{\partial\theta}{\partial x} + u_y \frac{\partial\theta}{\partial y} + u_z \frac{\partial\theta}{\partial z} \right) + \nabla \overline{w}^f \cdot \nabla\theta - \overline{w}^f G(|\dot{\gamma}|^*)^2 \eta^* \right] dD \right.$$

$$\left. - \int_{\Gamma_s} \overline{w}^f (\nabla\theta \cdot \mathbf{n}) d\Gamma_s \right\} dz = 0 \tag{19}$$

The shape functions are chosen to satisfy the boundary conditions on the barrel and must therefore vanish there.

Several approaches have been suggested in the literature for the definition of the perturbation function for SUPG. We have followed the method outlined by Hughes et al. In this analysis, an element in the arbitrary domain x, y, and z can be mapped into an isoparametric element of unit dimension in each of the transformed serendipity coordinates ξ, χ, and ζ. An element mesh parameter was then defined as

$$h^e = \frac{2\|\mathbf{u}\|}{b} \tag{20}$$

where ||**u**|| is the Euclidean norm of the velocities and b is given by

$$b^2 = \left(u_x \frac{\partial \xi}{\partial x} + u_y \frac{\partial \xi}{\partial y}\right)^2 + \left(u_x \frac{\partial \chi}{\partial x} + u_y \frac{\partial \chi}{\partial y}\right)^2 + \left(u_z \frac{\partial \zeta}{\partial z}\right)^2 \qquad (21)$$

Following Hughes et al. the perturbation function was taken as:

$$w^f = \frac{\sigma h^e \varepsilon^e}{2\|\mathbf{u}\|} \mathbf{u} \cdot \nabla W^f \qquad (22)$$

where,

$$\varepsilon^e = \coth \gamma^e - \frac{1}{\gamma^e} \text{ and } \gamma^e = Pe\|\mathbf{u}\|h^e/2 \qquad (23a, b)$$

NUMERICAL SOLUTION

Flow Equations

For the finite element solution of the momentum equations, the domain is discretized by bilinear elements in x and y and trial functions are chosen such that:

$$x^e = \sum_{i=1}^{Nod} x_i^e \pi_i^e(x,y) \qquad x_i^e, \pi_i^e \in D^e \qquad (24\ a, b)$$

where D^e is an element domain, Nod is the number of nodes per element and π_i^e is the trial function with x^e representing the velocity vector. The discretized equations take the matrix form:

$$\underline{\underline{\mathbf{A}}}\,\mathbf{x} = \mathbf{f} \qquad (25)$$

where $\underline{\underline{\mathbf{A}}}$ is the stiffness matrix and **f** is a force vector resulting from specified nodal values or source term and the nodal unknowns are recovered from the vector **x**.

Energy Equation

The shape functions for the temperature are similar to those used for velocity in that they are linear in the space coordinates. The weighting function W^f has a trilinear dependence on the x-, y-, and z- coordinates for regular flighted screw sections. Since the thermal problem is parabolic, the integration in z in Eq. 16 can be carried out independent of the other two directions producing a part with known values of θ (source term) and the other containing values of θ being sought. At this point, the solution procedure adopted for the velocity equations can then be applied.

The element mesh parameter h^e and the cell Peclet number γ^e in Eqs. 20 and 23 were evaluated based on the velocity at the centroid of the element. Our numerical experimentation revealed that the value of σ is dependent on such factors as the element skewness and the flow and heat transfer parameters.We have recommended that σ be adjusted until the solution is oscillation free. For the range of parameters considered in various case studies, the values of σ were between 0.5 and 3.0 and they furnished satisfactory results.

Solution Procedure

For regular flighted screw sections, at the inlet of the extrusion channel, the temperature distribution is known, hence only the x-, y-, and z- velocity components are computed, based on a specified value of the inlet pressure gradient dp_m^*/dz^*. The Picard iteration is then utilized for the shear rate dependent shear viscosity. After convergence, the volumetric flow rate is calculated. We proceed down the channel and as a first step, solve for the temperature distribution. With a viscosity distribution based on this temperature profile and the value of dp_m^*/dz^* at the previous channel location, for the second step, we solve for the velocity components and calculate the volumetric flow rate. A new value of dp_m^*/dz^* is obtained using the secant method with the residual taken as the difference between the calculated volumetric flow rate and that obtained at the inlet. This completes the second step which is repeated until convergence on account of shear rate dependent shear viscosity.

Subsequently, we solve for a new temperature distribution and go back to the second step since the shear viscosity material function is temperature dependent. This iterative procedure is continued until the volumetric flow rate constraint (Eq. 4) is satisfied and, simultaneously, the Euclidean norms of the

difference between successive iterates of **u** and θ are small, usually $\leq 10^{-3}$. Another step size is taken with the values of the variables at the previous channel location serving as the initial guesses. Convergence on the inner iteration for shear rate dependent shear viscosity is usually achieved in 4 to 8 iterations. On the other hand, the outer Picard iteration on account of the temperature coefficient of viscosity may require up to 10 iterations. The number of iterations depends on the channel location and the value of the temperature coefficient of viscosity. When the backflow is significant but not severe, the SUPG method provides reliable and accurate results when compared with the upwind marching scheme of finite difference, but the required number of iterations goes up slightly. The allowable step size, Δz, is dictated by the stability of the discretized temperature equation which is dependent on the thermal and flow parameters. The dimensionless step size used in this study is 1.0.

For the kneading disc sections of the twin screw extruder the full three-dimensional conservation equations need to be solved and the procedures used are more complicated. They are provided in detail in some of our publications (34, 37, 40, 41).

The typical role played by the viscoplasticity of highly filled materials on their continuous processability is demonstrated in Figures 15, 16. Here the suspension is pressurized in a co-rotating twin screw extruder [34, 37, 40-42]. The velocity distributions given in Figure 15 show that the flow is segregated into a high deformation rate region adjacent to the barrel surface and a low deformation rate zone away from the barrel. The consequence of this flow field is the formation of a hot spot adjacent to the barrel surface as shown in Figure 16, which needs to be avoided by proper selection of geometry and processing conditions.

An additional difficult aspect of continuous processing arises from the dispersive mixing associated with the exertion of high stress levels on small fractions of the suspension by forcing repeatedly through the small gaps found between screws or the screw and the barrel elements during continuous processing [34, 40]. This is illustrated in Figure 17 where high stress magnitudes are seen to be generated at such gaps during the processing of a viscoplastic suspension in a co-rotating twin screw extruder. The physical properties, including particle size distribution,

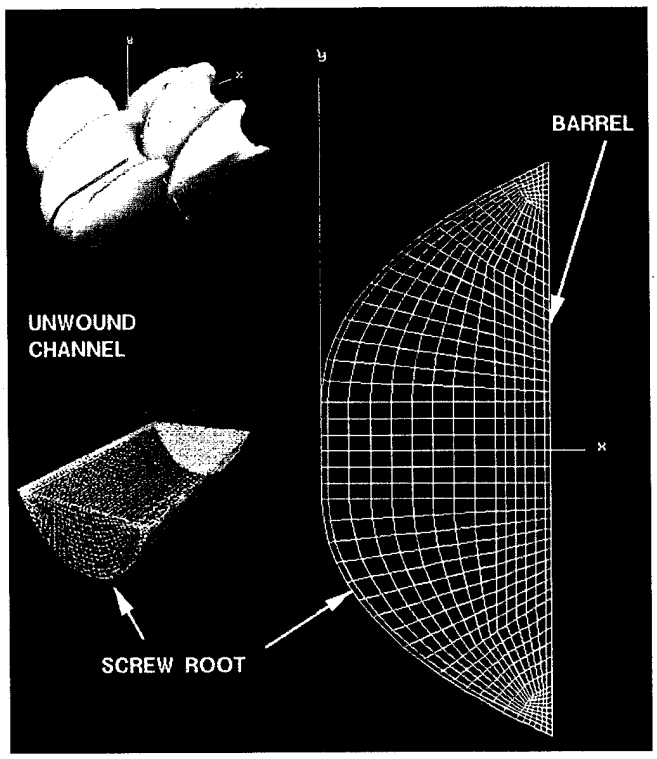

FINITE ELEMENT MESH

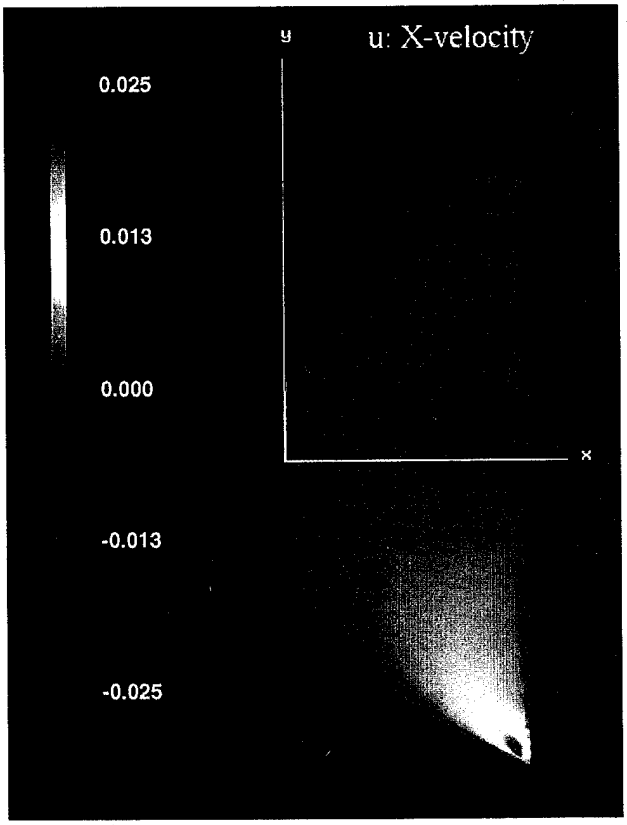

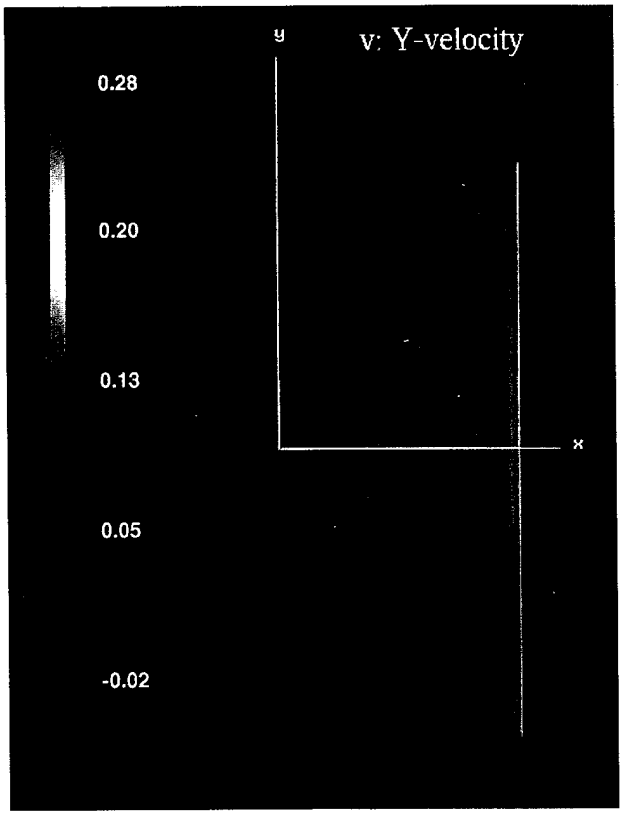

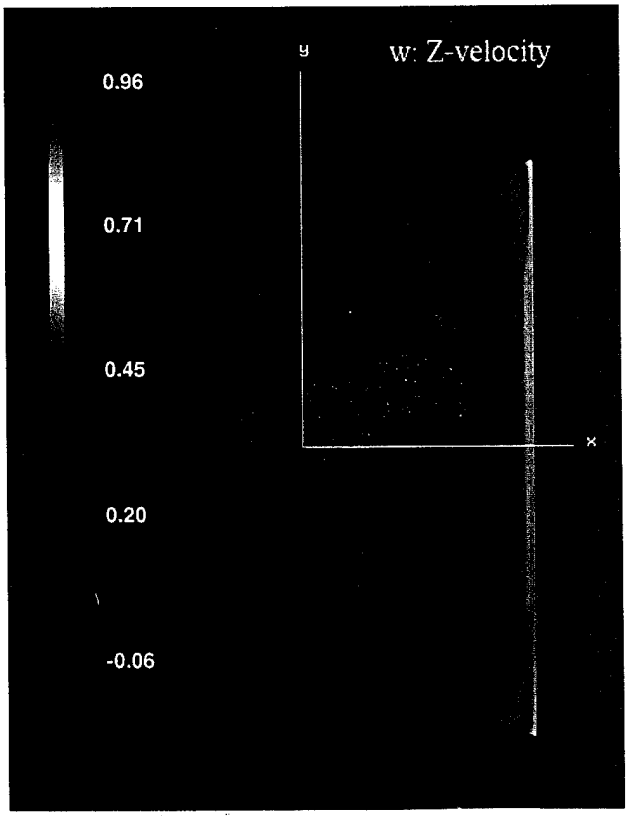

Figure 15. VELOCITY PROFILE

dp/dz axial = 1553 psi/ft; Q = 26 lb/hr

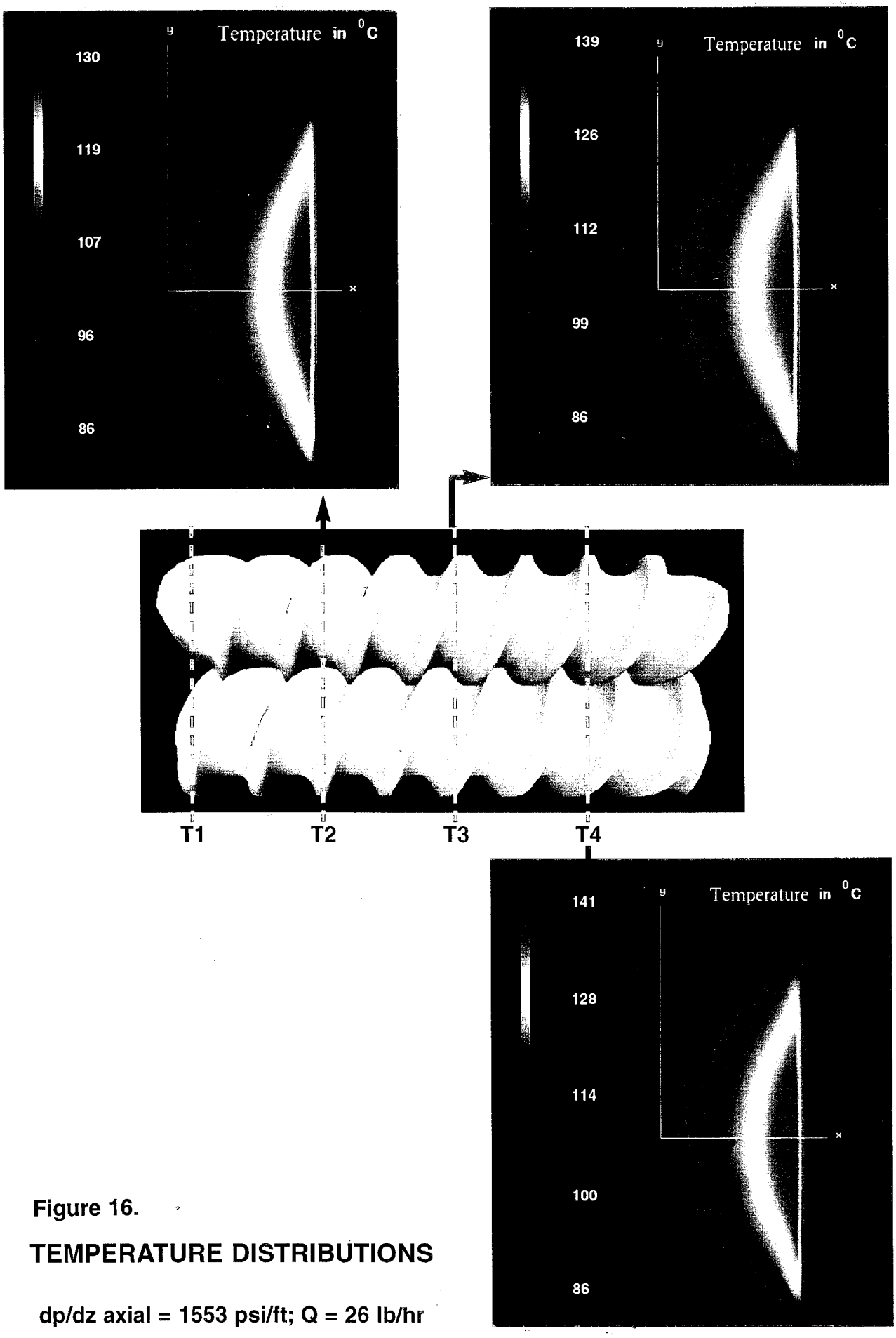

Figure 16.

TEMPERATURE DISTRIBUTIONS

dp/dz axial = 1553 psi/ft; Q = 26 lb/hr

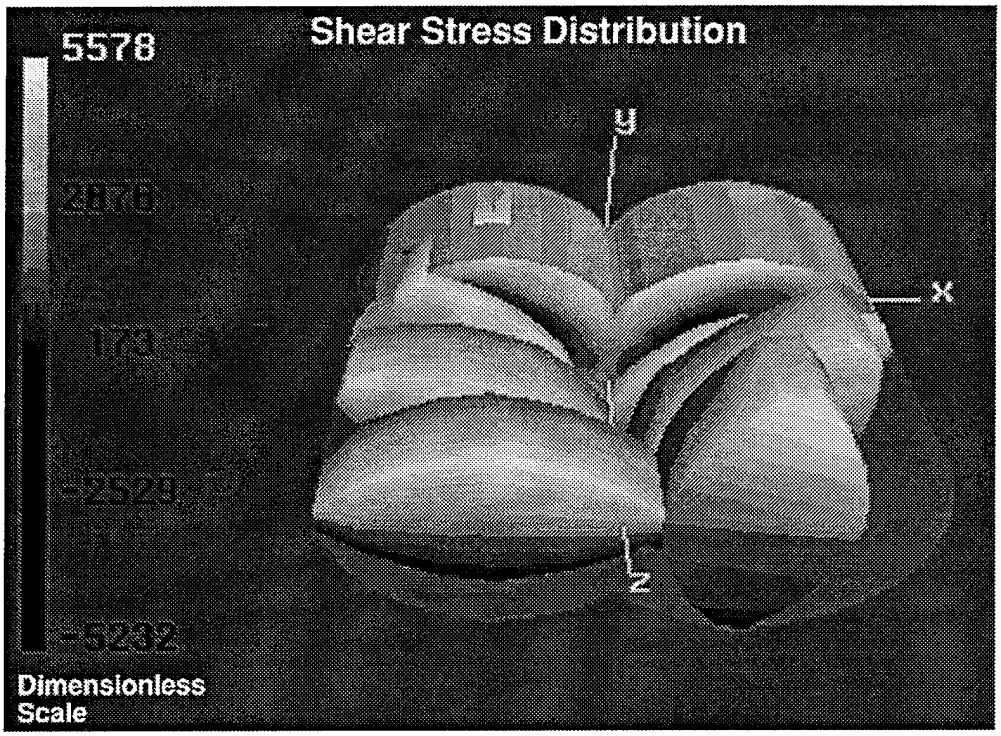

Figure 17. Distribution of the shear stress in a viscoplastic fluid being processed in the kneading disc region of a co-rotating twin screw extruder.

of the suspension experiencing the high stress region can become significantly different than the rest of the suspension.

Degree of Mixedness

Some of our experimental and numerical simulation techniques which were developed earlier with DARPA funding were subsequently applied to the investigation of propellant processing in co-rotating twin screw extrusion process using earlier funding provided by DARPA. Besides simulation technologies [36, 37, 40, 41], we have developed two experimental techniques which are both x-ray analysis based to characterize the volume ratio of various ingredients as a function of the scale of examination and location [43]. The techniques are illustrated in Figure 18 where the distributive mixing of a minor component indicated by a white blob in the geometry of two co-rotating kneading discs confined in a barrel is shown. On the other hand, we have also developed simulation techniques for predicting the degree of mixedness development in propellants during extrusion flow.

Figure 19 illustrates an x-ray based experimental technique, which we have developed [43]. The variation of the volume ratios of the binder, cellulose acetate butyrate, (CAB) over the solid content, i.e., RDX and HMX powders at various locations, are shown. Samples were either processed in a batch mixer and then ram extruded or processed and extruded in a twin screw extruder. Figure 20 shows that the volume fraction of the binder, CAB, is seen to vary considerably around the mean for the batch mixed sample versus the narrow distribution around the mean obtained with the continuously processed gun propellant sample. The difference becomes more significant at a smaller scale of examination i.e., at 1 mm^2. Predictions assume that the minor component is non-diffusive with no interfacial tension existing between the minor component and the remainder of the suspension [36]. As also experimentally observed, the distribution of the minor component in the remainder of the suspension becomes uniform with time [44]. We utilize the variance of the ratio of the minor to the major phases as a quantitative measure of degree of mixedness. The challenge is to determine proper locations for minor components to be input into the processor and selection of appropriate geometry and operating condition for efficient mixing without detoriating various properties of the suspension.

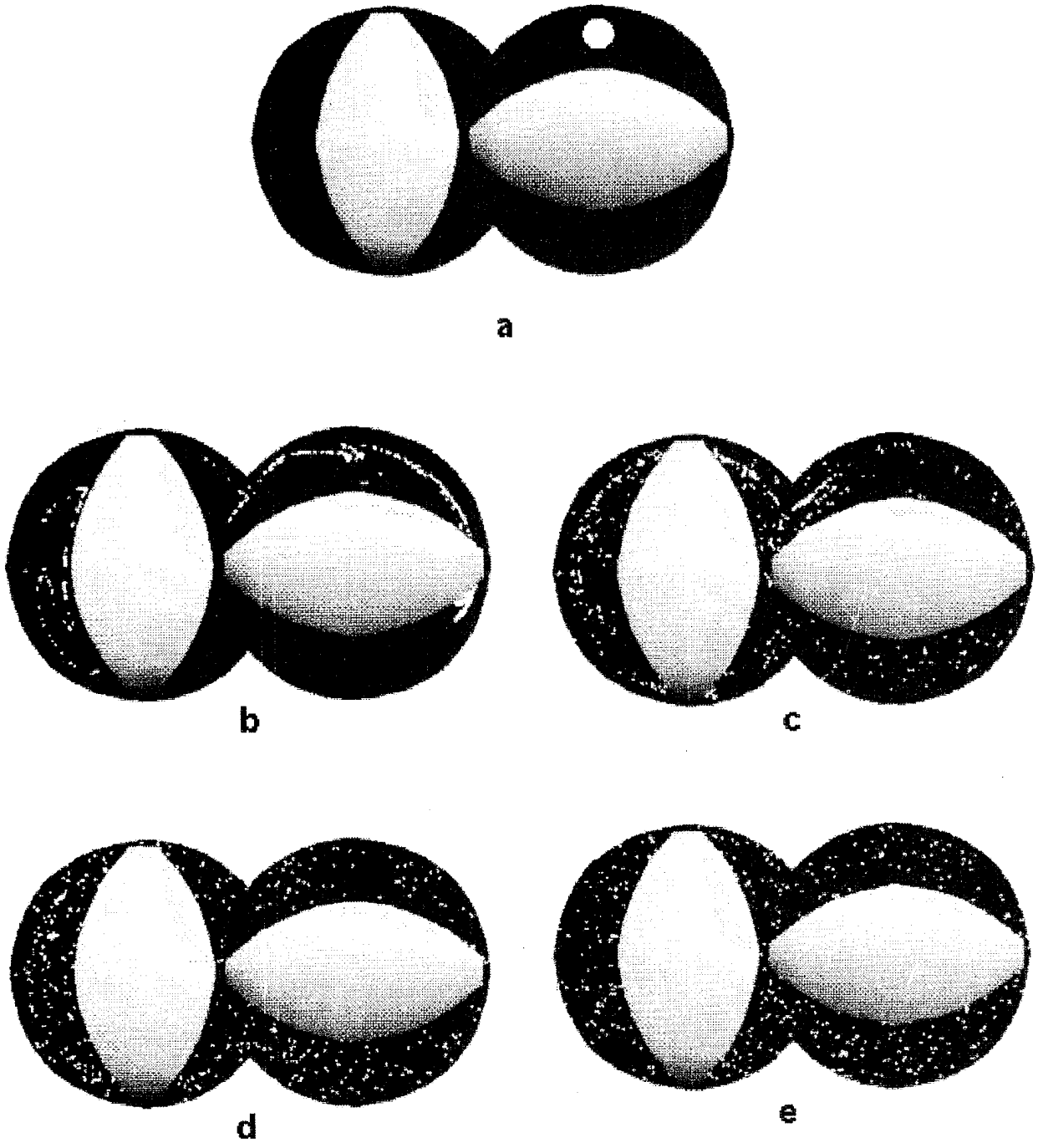

Figure 18. Distributive mixing of a non-diffusive passive tracer blob as a function of time, t, i.e., in periods of rotation, to, 2-D flow between two kneading disks [36]: a) t = 0; b) t = 2 periods; c) t = 5 periods; d) t = 10 periods; e) t = 20 periods.

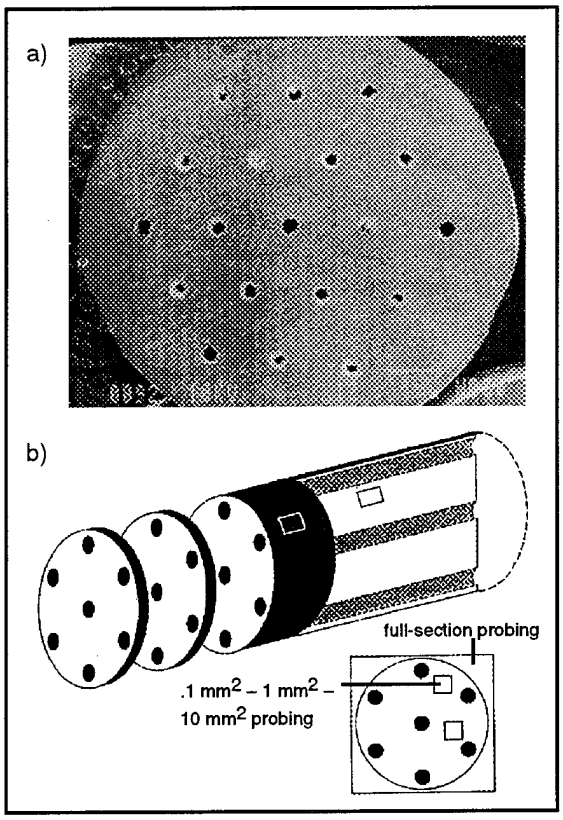

Figure 19. Extruded profile and sampling

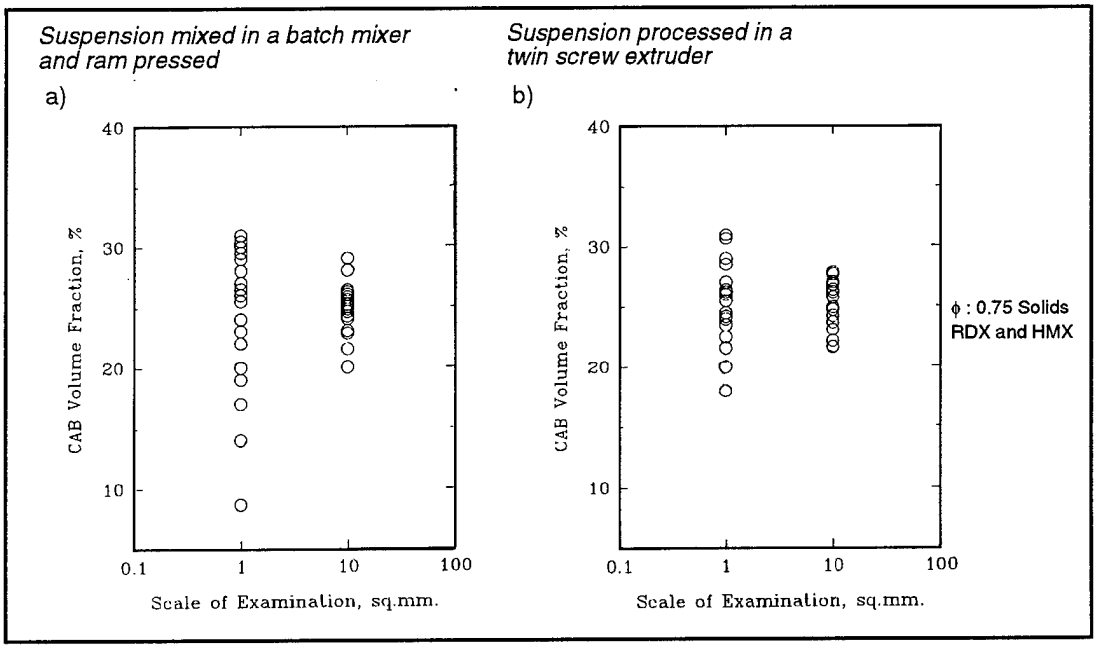

Figure 20. Quantitative analysis of degree of mixedness using the variance of the concentration of the binder, CAB, at two scales of examination for batch and continuously processed suspensions.

The mixing index values range from zero for a completely segregated sample (unmixed) to one for a perfect mixture with zero variance around the mean. The mixing index values for the batch mixed sample of Figure 20 is 0.85 and the twin screw processed sample is 0.92 at a scale of examination of 1 mm^2, indicating the superior distributive mixing capability of the twin screw extrusion process. This analysis technique and the simulation techniques for the first time allow the quantitative characterization of the degree of mixedness of suspension samples and facilitate the determination of proper mixing geometries and conditions for propellants in twin screw extrusion process.

Figure 21 shows the distribution of the tracer particles (numerical tracer i.e., absence of interfacial effects) initially forming a coherent blob located at the entry point of a kneading disc section of the co-rotating twin screw extruder. The rapid redistribution of the tracer particles with increasing residence time in the kneading section was characterized by the first solution of the time-dependent velocity distributions in the kneading disc section followed by determination of particle paths.

Figure 22 shows the typical residence time distribution plots for various kneading disc configuration in the co-rotating twin screw extrusion process. The effect of decreasing of the stagger angle is to increase the breadth of the residence time distribution. The short residence time values at 30^o stagger are indicative of the "pipeline" flows (which were also experimentally observed for 30^o) and the long residence times support the formation of relatively stagnant regions in the extruder.

VIII. **Free Surface Flows**

A number of sections of the twin screw extruder operate on the basis of partially-full mode. This is typically shown in Fig. 23 where the degree of fill changes with the geometry employed (increase with reversely configured sections and decrease as the stagger angle decreases for forwardly configured screw sections). For the regular flighted screw sections, the partially full section only serves as a conveying geometry with little/no distributive or dispersive mixing of the ingredients. The degree of fill in such sections and the residence time can be

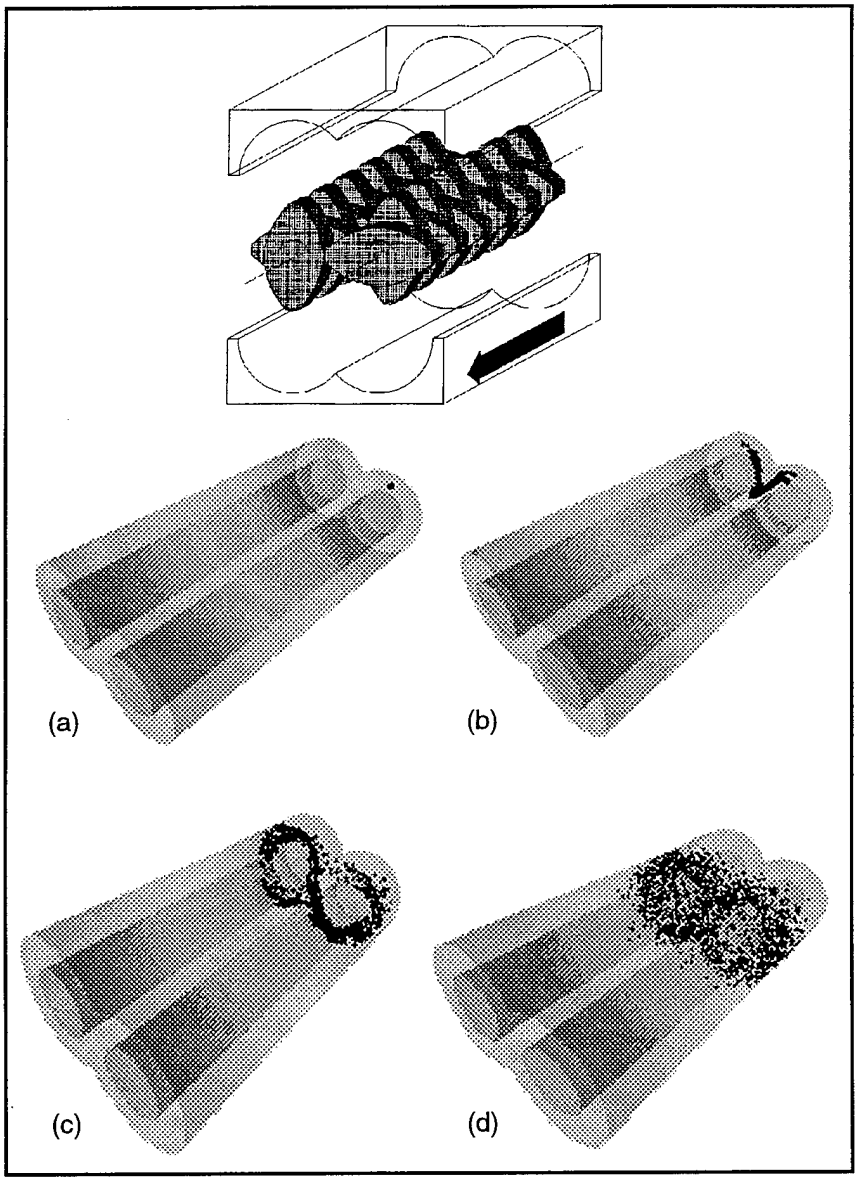

Figure 21. Mixing of a blob for kneading discs staggered at 90° netural: (a) t = 0, (b) t = T_o, (c) = $5T_o$, and (d) t = $20T_o$ neutral.

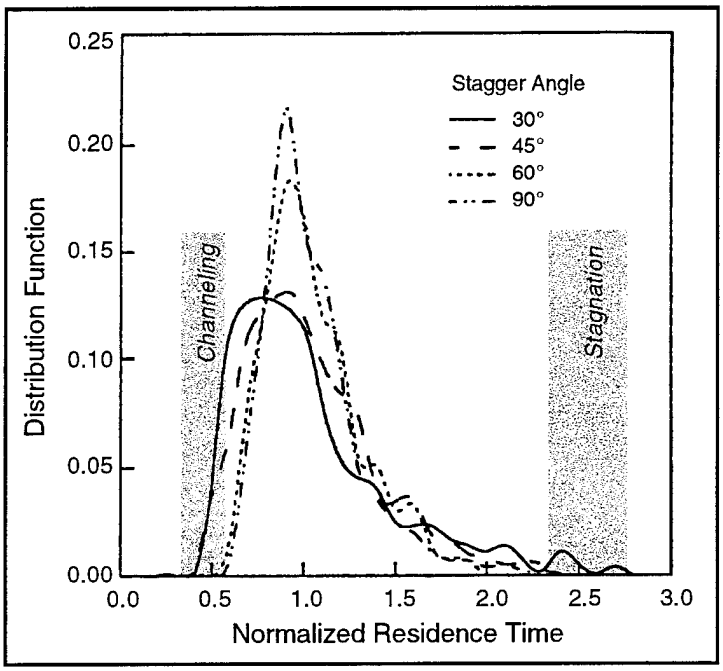

Figure 22. The comparison of the residence time distribution functions generated by kneading disc screw sections staggered at 30°, 45°, 60° forward, and 90° neutral.

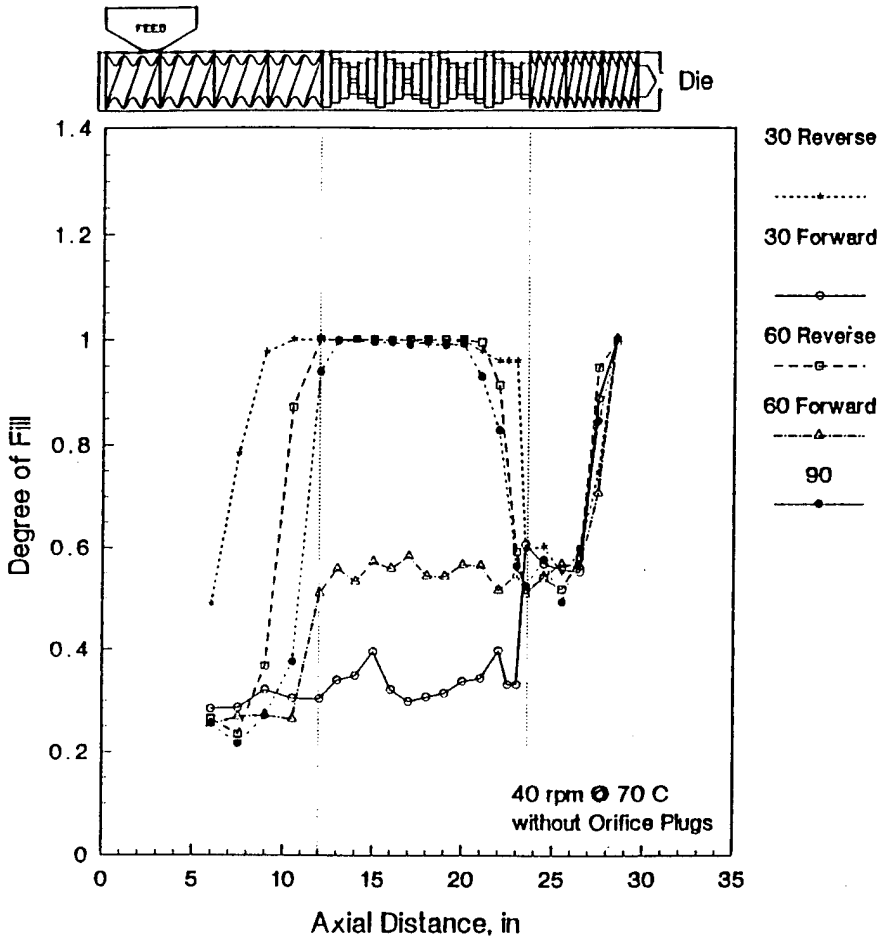

Figure 23. Degree of fill distribution with various kneading disc stagger angles at 70°C and 40 rpm.

determined easily since the volumetric flow rate for pure-drag flow is not a function of the rheological behavior of the suspension nor the wall slip condition.

On the other hand, the partially-full sections in the kneading disc sections cannot be modeled with the present state of knowledge. In such sections, the motion is governed by chaotic dynamics with positive Lyapunov exponents and characterized by absolute dependence on the initial condition.

The regular flighted screw sections found in the devolatilization section are where the mass transfer area i.e., interfacial area between air/vacuum and the suspension is important. We have applied the "method of spines" technique developed by Prof. Scriven and co-workers to determine the shape of the free surface as a function of surface tension, contact angles and wall slip coefficient of the suspension on the extruder surfaces. Typical results for x-and z-velocity (transverse and down-channel directions) are shown in Figure 24, where the free surface is indicated. The determination capability of the free surface shape, however, does not immediately translate to a devolatilization model, since the nucleation and growth of bubbles and their collapse during devolatilization are phenomena which are hitherto not mathematically modeled. We have attempted such a model in conjunction with development of pore formation in conversion of polymeric precursors to ceramics (Ref´ns 46), but had no opportunity to adapt and carry-over to devolatilization process.

The ramifications of all these findings and capabilities to the BMDO program in terms of reducing the safety risk in continuous processing and optimization of the process towards "total quality management" through the understanding generated and the numerical/experimental tools developed are discussed next.

IX. Conclusions and Ramifications

1. The flow and deformation behavior of propellants is affected by the formation of a binder-rich region adjacent to the wall i.e., wall slip region. Generally, the energetic suspension flows like a plug (solid-like), lubricated at the wall with the slip region adjacent to the wall.

Mathematical modeling of 2-D free surface flows using "method of spines."

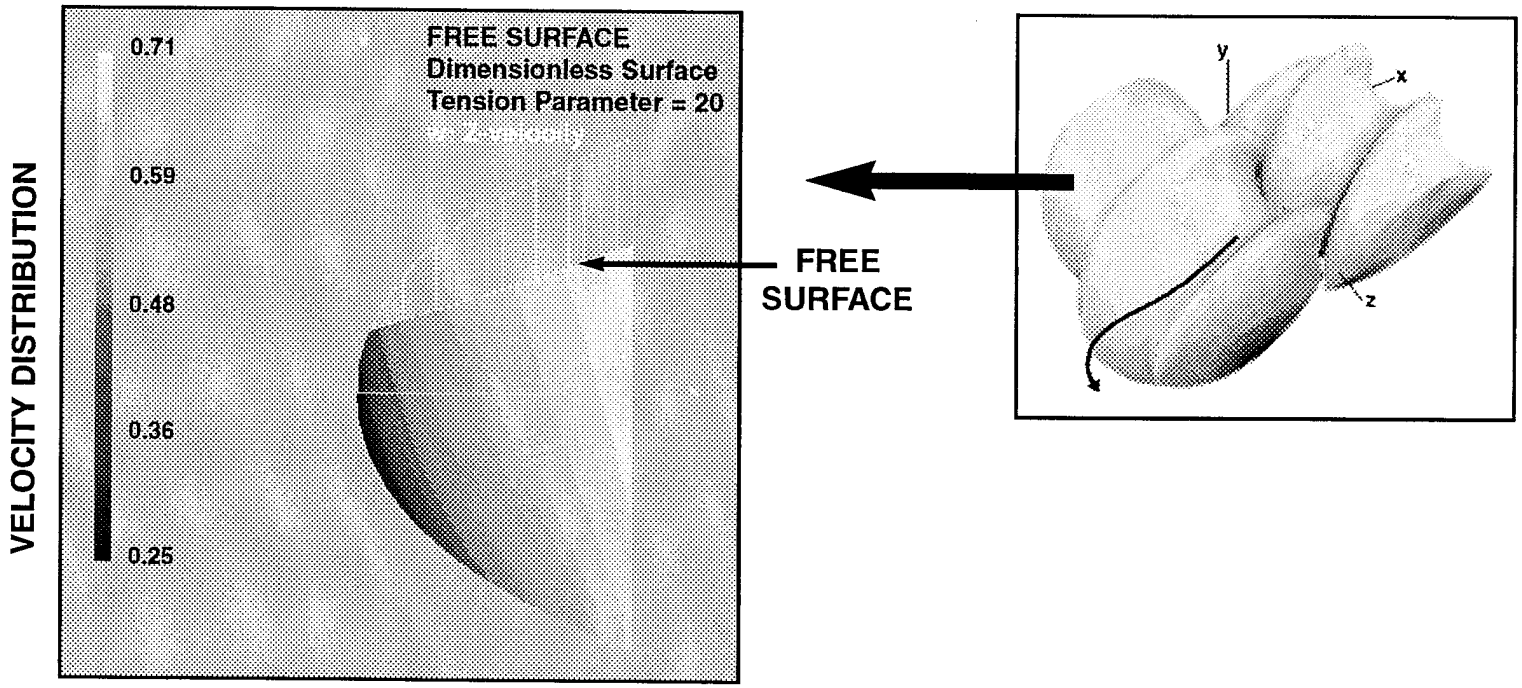

SIT's mathematical model:

- **Determines free surface shape in 2-D flows**
- **Predicts the velocity, stress and temperature distributions in partially full channel**

Fig. 24-A

Circulatory flow in the Twin Screw Extruder

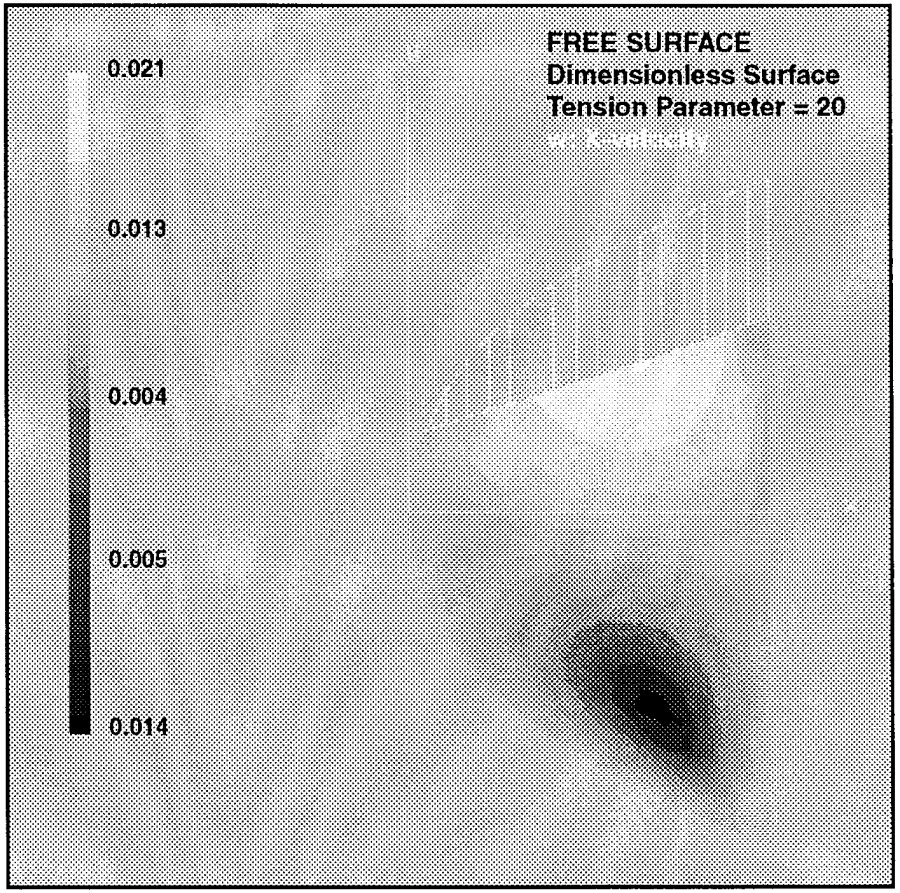

- FEM simulation shows the circulatory flow in partially full channel
- The circulatory flow induces surface renewal at free surface to facilitate mass transfer of air and solvents out of propellant

Fig. 24-B

2. The solid-like behavior of propellants in various flow regimes renders their processing in twin screw extrusion processing i.e., mixing and pressurization and, shaping in dies and molds a challenge.

3. On-line analysis techniques attempting to probe various chemical or physical aspects of propellants should be able to penetrate beyond the wall slip layer to characterize the flowing suspension.

4. The thickness of the deforming slip layer changes as a function of binder and solid phase characteristics of the propellant.

5. Plug-like flow of the propellant occurs at low wall shear stress values for shear thinning propellant formulations with multimodal size particles and at high wall shear stress values for shear thickening propellant, with narrow particle size distributions.

6. Formation of solid-like plugs with lubrication layers at the wall renders it difficult to achieve adequate mixing and processing of propellants requiring specialized mixing and dispersion elements in twin screw extrusion.

7. The microstructure of the propellant suspension evolves continuously as a function of flow and deformation history. Microstructure development encompasses migration of particles based on shear rate and concentration gradients, interlocking of particles to form solid-like plugs, encapsulation of binder locally upon interlocking, formation of binder-rich layers at high shear rate regions, entrainment of air/solvent gases, and lubrication of surfaces with air/gases.

8. Especially with propellant suspensions containing low viscosity binders, the binder migrates in the direction of the overall pressure gradient, with such filtration superimposed on the bulk flow of the propellant suspension. This migration results in the demixing of the propellant upon pressurization in die and mold flows and leads to cyclic, mat-formation based flow instabilities.

9. The factors involved in binder migration and development of flow instabilities are understood, with major effects arising from degree of channel

convergence, particle diameter, and binder viscosity. Binder migration during propellant processing should be minimized to eliminate the formation of stagnant solid regions in processors, particle attrition, quality problems and increasing safety risks during continuous processing.

10. Attempts to eliminate wall slip during deformation by roughening the walls of processors generate fracture surfaces (discontinuities of velocity) in propellants.

11. The development of wall slip behavior of propellants during deformation is time and temperature dependent.

12. The peculiarities of the flow and deformation behavior of propellant suspensions with their high degree of fill require specialized numerical analysis techniques for mathematical modeling of their processability in twin screw extrusion process which especially incorporate the wall slip behavior.

13. The wall slip behavior of propellant suspensions can be characterized in viscometric flows and used for first-order analysis of 2-D and 3-D processing flows as an interfacial dynamic boundary condition.

14. The rheological behavior of the propellant suspensions is especially affected by the presence of a gaseous phase i.e., air or solvents and is altered significantly upon their removal. The gas entrainment characteristics of the propellant suspension differs significantly at different locations in a continuous processor especially varying between the partially-full and completely full sections of the twin screw extruder.

15. The wall slip behavior and hence processability of propellant suspensions can be affected to some extent by the choice of materials of construction with different material use on moving and stationary surfaces of the twin screw extruder, being the most effective.

16. The microstructure of propellant suspensions which controls their flow and deformation behavior as well as their various ultimate properties like burning rate and mechanical properties are affected foremost by the degree of

interspersing of various ingredients of the formulation and the physical properties of the ingredients (such as particle size of solids which can change during processing).

17. On-line rheometers for highly filled materials such as propellants should be able to probe at a number of deformation rates without significantly altering the microstructure of the suspension.

18. The axial migration of binder in converging flow generally prevents the use of gear pumps and sensors where suspension is dragged into small clearances for highly filled materials.

19. Small changes in characteristics of raw ingredients such as particle size and shape of the solid phase of propellant suspensions where the intended solid volume concentration approaches the maximum packing fraction may result in suspensions which are not processable (for example arising from the segregation of sold ingredients according to size or density in bins and hoppers).

20. X-ray based techniques developed earlier could be also applied to characterize the degree of mixedness of suspensions processed in co-rotating twin screw extrusion process.

21. The processability of concentrated suspensions could be simulated assuming a continuum by solving the conservation equations using 2-D and 3-D Finite Element Method.

22. The mixing effectiveness of twin screw extrusion geometries and operating conditions could be quantitatively assessed using tools of dynamics employing non-diffusive numerical tracers.

23. The generic understanding gained by applying multi-disciplinary studies on propellants and their simulants is also relevant to other materials encountered in multiple industries relevant to Navy.

24. New technologies can be developed or existing technologies improved by understanding the generic nature of propellant-like materials which are filled very close to their maximum packing fraction.

Acknowledgments

We acknowledge the support of Ballistic Missile Defense Organization, Innovative Science and Technology Office as managed by ONR, which made the findings reported here possible. We thank Dr. Richard S. Miller of ONR for his continuous guidance and encouragement. The members of my research group who have contributed to the findings summarized here are listed in the publications.

REFERENCES

1. J. V. Milewski, "A Study of the Packing of Fibers and Spheres", Ph.D. Thesis, Rutgers University, N.J. (1973).

2. N. Ouchiyama and T. Tanaka, *Ind. Eng. Chem. Fund., 19,* 338 (1980) also *20,* 66 (1981) and *23,* 490 (1984).

3. T. Fiske, S. Railkar and D. M. Kalyon, "Effects of Segregation on the Packing of Spherical and Non-Sypherical Particles," *Powder Technology, 81* (1994) 57-64.
4. M. Mooney, "Explicit Formulas for Slip and Fluidity", *J. Rheol., 2,* 210-222 (1931).

5. V. Vand, "Viscosity of Solutions and Suspensions," *J. Phys. Coll. Chem., 52,* 277 (1948).

6. Y. Cohen and A. Metzner, "Apparent Slip Flow of Polymer Solutions," *J. Rheol., 29,* 67 (1985).

7. A. Yoshimura and R. Prud'homme, "Wall Slip Corrections for Couette and Parallel Disk Viscometers," *J. Rheol., 32,* 53 (1988).

8. D. M. Kalyon and U. Yilmazer, "Rheological Behavior of Highly Filled Suspensions Which Exhibit Slip at the Wall," *Polymer Rheology and Processing,* A. Collyer and L. Utracki, eds., Elsevier Applied Science, London (1990).

9. U. Yilmazer and D. M. Kalyon, "Slip Effects in Capillary and Parallel Disk Torsional Flows of Highly Filled Suspensions," *J. Rheology, 33,* 8 (1989) 1197-1212.

10. D. M. Kalyon, B. Aral and U. Yilmazer, "Rheological Behavior of Highly Filled Suspensions," *Society of Plastics Engineers, ANTEC Technical Papers, 36* (1990) 1560-1564.

11. Y. Chen, D. M. Kalyon and E. Bayramli, "Wall Slip Behavior of Linear Low Density Polyethylene in Capillary Flow: Effects of Materials of Construction and Surface Roughness," *Society of Plastics Engineers ANTEC Technical Papers, 38* (1992) 1747-1751.

12. U. Yilmazer and D. M. Kalyon, "The Role of Interface at the Wall in Flow of Concentrated Composites," *The Interfacial Interactions in Polymeric Composites,* NATO Advanced Study Institute, G. Akovali, ed., Antalya, Turkey, 1992.

13. D. M. Kalyon, P. Yaras, B. Aral and U. Yilmazer," Rheological Behavior of Concentrated Suspensions: A Solid Rocket Fuel Simulant," *J. Rheology,* 37 (1993) 35-53.

14. D. M. Kalyon, "Review of Factors Affecting the Continuous Processing and Manufacturability of Highly Filled Suspensions," *Journal of Materials Processing and Manufacturing Science, 2* (1993), 159-187.

15. Y. Chen, D. M. Kalyon and E. Bayramli, "Effects of Surface Roughness and the Chemical Structure of Materials of Construction on Wall Slip Behavior of Linear Low Density Polyethylene in Capillary Flow," *J. Appl. Polym. Sci., 50* (7), (1993) 1169-1177.

16. B. Aral and D. M. Kalyon, "Effects of Temperature and Surface Roughness on Time-Dependent Development of Wall Slip in Torsional Flow of Concentrated Suspensions," *J. of Rheol. (38) 4,* (1994) 957-972.

17. U. Yilmazer and D. M. Kalyon, "Dilatancy of Concentrated Suspensions with Newtonian Matrices," *Polymer Composites 12,* 4 (1991) 226-232.

18. A. Karnis, H. Goldsmith and S. Mason, "Axial Migration of Particles in Poiseuille Flow", *Nature, 200,* 159-160 (1963).

19. O. Leighton and A. Acrivos, "The Shear Induced Migration of Particles in Concentrated Suspensions", *J. Fluid Mech., 181,* 415-439 (1987).

20. R. Phillips, R. Armstrong, R. Brown, A. Graham and J. Abbott, "A Constitutive Equation for Concentrated Suspensions that accounts for Shear-Induced Particle Migration", *Phys. Fluids, A,* 30-40 (1992).

21. U. Yilmazer, C. G. Gogos and D. M. Kalyon, "Unstable Flows During Compounding of Highly Filled Suspensions," *Society of Plastics Engineers ANTEC Technical Papers, 35* (1989) 191-195.

22. U. Yilmazer , C. Gogos and D. M. Kalyon, "Mat Formation and Unstable Flows of Highly Filled Suspensions in Capillaries and Continuous Processors," *Polymer Composites, 10,* 4 (1989) 242-248.

23. P. Yaras, U. Yilmazer and D. M. Kalyon, "Unstable Flow of Concentrated Suspensions in Tube Flow," *Society of Plastics Engineers ANTEC Technical Papers, 39* (1993) 2604-2606.

24. P. Yaras, D. M. Kalyon, and U. Yilmazer, "Flow Instabilities in Capillary Flow of Concentrated Suspensions," *Rheologica Acta,* 33, (1994) 48-59.

25. J. W. Sinton, J. C. Crowley, G. A. Lo, D. M. Kalyon and C. Jacob, "Nuclear Magnetic Resonance Imaging Studies of Mixing in Twin Screw Extruders," *Society of Plastics Engineers, ANTEC Technical Papers, 36* (1990) 116-119.

26. D. M. Kalyon, C. Jacob and P. Yaras, "An Experimental Study of the Degree of Fill and Melt Densification in Fully-intermeshing, Co-rotating Twin Screw Extruders," *Plastics, Rubber and Composites Processing and Applications, 16,* 3 (1991) 193-200.

27. D. M. Kalyon, R. Yazici, C. Jacob, B. Aral and S. W. Sinton, "Effects of Air Entrainment on the Rheology of Concentrated Suspensions during Continuous Processing," *Polym. Eng. Sci., 31* (1991) 1386-1392.

28. B. Aral, D. M. Kalyon and H. Gokturk, "The Effects of Air Incorporation in Concentrated Suspension Rheology," *Society of Plastics Engineers ANTEC Technical Papers, 38* (1992) 2448-2451.

29. B. Aral and D. M. Kalyon, "Rheology and Extrudability of Very Concentrated Suspensions: Effects of Vacuum Imposition," submitted to *Plast. and Rubber Comp. Proc. and Applications,* 1994.

30. D.M. Kalyon, H. Gokturk, P. Yaras and B. Aral, "Motion Analysis of Development of Wall Slip During Die Flow of Concentrated Suspensions," accepted to appear in *SPE ANTEC Technical Papers* (1995).

31. D. M. Kalyon, "Mixing in Continuous Processors," *Encyclopedia of Fluid Mechanics, 7,* Gulf Publishing (1988) Chapter 28, pp. 887-926.

32. A. Lawal and D. M. Kalyon, "Single Screw Extrusion of Viscoplastic Fluids Subject to Different Slip Coefficients at Screw and Barrel Surfaces," *Polym. Eng. Sci., 34* (1994) 1471-1479.

33. Z. Ji, A. Gotsis and D. M. Kalyon, "Single Screw Extrusion Processing of Highly Filled Suspensions Including Wall Slip," *Society of Plastics Engineers, ANTEC Technical Papers, 36* (1990) 160-163.

34. A. D. Gotsis, A. Ji and D. M. Kalyon, "3-D Analysis of the Flow in Co-rotating Twin Screw Extruders," *Society of Plastics Engineers, ANTEC Technical Papers, 36* (1990) 139-142.

35. A. Lawal and D. M. Kalyon, "Incorporation of Wall Slip in Non-isothermal Modeling of Single Screw Extrusion Processing," *Proceedings of the First International Conference on Transport Phenomena in Processing,* S. Guceri, ed., Technomic Publ. Co. (1992) 985-996.

36. A. Lawal, Z. Ji and D. M. Kalyon, "Computational Study of Chaotic Mixing in Co-Rotating Two-Tipped Kneading Paddles: Two-Dimensional Approach," *Polymer Engineering and Science,* 33, (3), (1992) 140-148.

37. A. Lawal and D. M. Kalyon, "Three Dimensional Analysis of Co-rotating Twin Screw Extrusion Using Tools of Dynamics," *Society of Plastics Engineers ANTEC Technical Papers, 39* (1993) 3397-3400.

38. A. Lawal, D. M. Kalyon and U. Yilmazer, "Extrusion and Lubrication Flows of Viscoplastic Fluids with Wall Slip," *Chem. Eng. Comm., 122* (1993) 127.

39. A. Lawal and D. M. Kalyon, "A Non-isothermal Model of Single Screw Extrusion of Generalized Newtonian Fluids," *Numerical Heat Transfer, 26* (1), (1994) 103-121.

40. A. Lawal and D. M. Kalyon, "Mechanisms of Mixing in Single Screw and Co-rotating Twin Screw Extruders," *Polym. Eng. Sci.,* 35, 17 (1995) 1325-1338.

41. A. Lawal and D. M. Kalyon, "Simulation of the Intensity of Segregation Distributions Using Three-Dimensional FEM Analyses: Applications to Co-rotating Twin Screw Extruders, *Journal of Applied Polymer Science,* (1995).

42. D. M. Kalyon, A. Gotsis, U. Yilmazer, C. Gogos, H. Sangani, B. Aral and C. Tsenoglou, "Development of Experimental Techniques and Simulation Methods to Analyze Mixing in Co-rotating Twin Screw Extrusion," *Advances in Polymer Technology, 8,* 4 (1988) 337-353.

43. R. Yazici and D. M. Kalyon, "Degree of Mixing Analyses of Concentrated Suspensions by Electron Probe and X-Ray Diffraction," *Rubber Chem. and Techn., 66* (4), (1993) 527-537.

44. D. M. Kalyon and H. Sangani, "An Experimental Study of Distributive Mixing in Fully Intermeshing Co-rotating Twin Screw Extruders," *Polymer Engineering Science, 29,* 15 (1989) 1018-1026.

45. D. M. Kalyon and H. S. Gokturk, "Adjustable Gap Rheometer," U.S. Patent and Trademark Office; # 5277058; issued on Jan. 11, 1994.

46. H. Yao, S. Kovenklioglu and D. M. Kalyon, "Pore Formation in the Pyrolysis of Polymers to Ceramics," Chem. Eng. Comm., 96, (1990) 155-175.

APPENDIX

Listing of publications in various areas emanating from BMDO/IST grant as managed by ONR

Our contributions in various areas emanating principally or partially from our SDIO/IST (BMDO/IST) are reported in the following publications:

A) Rheological Behavior

1. D. M. Kalyon and U. Yilmazer, "Rheological Behavior of Highly Filled Suspensions which Exhibit Slip at the Wall," Polymer Rheology and Processing, A. Collyer and L. Utracki, eds., Elsevier Applied Science, London (1990).

2. C. Tsenoglou, D. M. Kalyon and C. Gogos, "A Viscoelastic Constitutive Relationship in Flowing Polymer Suspensions and Composites," Engineering Applications of New Composites, Oxon, U.K. (1988).

3. U. Yilmazer and D. M. Kalyon, "Slip Effects in Viscometric Flows of Highly Filled Suspensions," Society of Plastics Engineers ANTEC Technical Papers, 35 (1989) 1682-1686.

4. U. Yilmazer, C. G. Gogos and D. M. Kalyon, "Unstable Flows During Compounding of Highly Filled Suspensions," Society of Plastics Engineers ANTEC Technical Papers, 35 (1989) 191-195.

5. U. Yilmazer, C. Gogos and D. M. Kalyon, "Mat Formation and Unstable Flows of Highly Filled Suspensions in Capillaries and Continuous Processors," Polymer Composites, 10, 4 (1989) 242-248.

6. U. Yilmazer and D. M. Kalyon, "Slip Effects in Capillary and Parallel Disk Torsional Flows of Highly Filled Suspensions," J. Rheology, 33, 8 (1989) 1197-1212.

7. D. M. Kalyon, B. Aral and U. Yilmazer, "Rheological Behavior of Highly Filled Suspensions," Society of Plastics Engineers, ANTEC Technical Papers, 36, (1990) 1560-1564.

8. U. Yilmazer and D. M. Kalyon, "Dilatancy of Concentrated Suspensions with Newtonian Matrices," Polymer Composites 12, 4 (1991) 226-232.

9. D. M. Kalyon, R. Yazici, C. Jacob, B. Aral and S. W. Sinton, "Effects of Air Entrainment on the Rheology of Concentrated Suspensions During Continuous Processing," Polym. Eng. Sci., 31 (1991) 1386-1392.

10. B. Aral, D. M. Kalyon and H. Gokturk, "The Effects of Air Incorporation in Concentrated Suspension Rheology," Society of Plastics Engineers ANTEC Technical Papers, 38 (1992) 2448-2451.

11. D. Kalyon, "Rheological Behavior of Highly Filled Suspensions," Proceedings of Joint Ordnance Commanders Group, 6th Annual Meeting of the Continuous Extruder and Mixer Users Group, sponsored by US Army and Navy, Phoenix, AZ, Nov. 17, 1992.

12. U. Yilmazer and D. M. Kalyon, "The Role of Interface at the Wall in Flow of Concentrated Composites," The Interfacial Interactions in Polymeric Composites, NATO Advanced Study Institute, G. Akovali, ed., Antalya, Turkey, 1992.

13. B. Aral and D. M. Kalyon, "Time-Dependent Development of Wall Slip in Shear Flows of Concentrated Suspensions," Society of Plastics Engineers ANTEC Technical Papers, 39 (1993) 2607-2610.

14. P. Yaras, U. Yilmazer and D. M. Kalyon, "Unstable Flow of Concentrated Suspensions in Tube Flow," Society of Plastics Engineers ANTEC Technical Papers, 39 (1993) 2604-2606.

15. D. M. Kalyon, P. Yaras, B. Aral and U. Yilmazer, "Rheological Behavior of Concentrated Suspensions: A Solid Rocket Fuel Simulant," J. Rheology, 37 (1993) 35-53.

16. D. M. Kalyon, U. Yilmazer, B. Aral and P. Yaras, "Rheological Behavior of Solid Rocket Fuel Simulants," Proceedings of 1993 JANNAF Propellant Development and Characterization Subcommittee Meeting, Livermore, CA, April 29, 1993.

17. P. Yaras, D. M. Kalyon, and U. Yilmazer, "Flow Instabilities in Capillary Flow of Concentrated Suspensions," Rheologica Acta, 33, (1994) 48-59.

18. B. Aral and D. M. Kalyon, "Effects of Temperature and Surface Roughness on Time-Dependent Development of Wall Slip in Torsional Flow of Concentrated Suspensions," J. of Rheol. (38) 4, (1994) 957-972.

B) PROCESSING

19. D. M. Kalyon, "Mixing in Continuous Processors," *Encyclopedia of Fluid Mechanics, 7,* Gulf Publishing (1988) Chapter 28, pp. 887-926.

20. D. M. Kalyon, "Applications of Continuous Mixers," *Encyclopedia of Engineering Materials,* N. Cheremisinoff, ed., Marcel Dekker (1988).

21. D. M. Kalyon, J. Yu and C. Du, "A Distributed Model of Flow in spiral Mandrel Die," *Polymer Process Engineering, 5,* 2 (1987) 179-207.

22. D. M. Kalyon, "Pressurization and Pumping in Polymer Processing," *Chemical Engineering Progress,* June (1987) 48-51.

23. D. M. Kalyon, "Melting, Softening and Solidification in Polymer Processing," *Chemical Engineering Progress,* June (1987) 45-48.

24. D. M. Kalyon, "Handling of Particulate Solids," *Chemical Engineering Progress,* June (1987) 42-45.

25. D. M. Kalyon, A. Gotsis, C. Gogos and C. Tsenoglou, "Towards a Better Understanding of Mixing in Co-rotating Twin Screw Extruders," *Society of Plastics Engineers ANTEC Technical Papers, 34* (1988) 64-66.

26. D. M. Kalyon, A. Gotsis, C. Gogos and C. Tsenoglou, "Simulation of the Mixing of Highly Filled Suspensions in the Co-rotating Twin Screw Extrusion Process," *Innovative Science and Technology Symposium of SPIE, Propulsion* (1988) 71-78.

27. D. M. Kalyon, A. Gotsis, U. Yilmazer, C. Gogos, H. Sangani, B. Aral and C. Tsenoglou, "Development of Experimental Techniques and Simulation Methods to Analyze Mixing in Co-rotating Twin Screw Extrusion," *Advances in Polymer Technology, 8,* 4 (1988) 337-353.

28. A. D. Gotsis and D. M. Kalyon, "Simulation of Mixing in Co-rotating Twin Screw Extruders," *Society of Plastics Engineers ANTEC Technical Papers, 35* (1989) 44-48.

29. D. M. Kalyon and H. N. Sangani, "Characterization of Distributive Mixing in Fully-Intermeshing, Co-rotating Twin Screw Extruders," *Society of Plastics Engineers ANTEC Technical Papers, 35* (1989) 124-128.

30. D. M. Kalyon and H. Sangani, "An Experimental Study of Distributive Mixing in Fully Intermeshing Co-rotating Twin Screw Extruders," *Polymer Engineering Science, 29,* 15 (1989) 1018-1026.

31. Z. Ji, A. Gotsis and D. M. Kalyon, "Single Screw Extrusion Processing of Highly Filled Suspensions Including Wall Slip," *Society of Plastics Engineers, ANTEC Technical Papers, 36* (1990) 160-163.

32. A. D. Gotsis, A. Ji and D. M. Kalyon, "3-D Analysis of the Flow in Co-rotating Twin Screw Extruders," *Society of Plastics Engineers, ANTEC Technical Papers, 36* (1990) 139-142.

33. D. M. Kalyon, C. Jacob and P. Yaras, "An Experimental Study of the Degree of Fill and Melt Densification in Fully-intermeshing, Co-rotating Twin Screw Extruders," *Plastics, Rubber and Composites Processing and Applications, 16,* 3 (1991) 193-200.

34. Z. Ji and D. M. Kalyon, "Two Dimensional Computational Study of Chaotic Mixing in Two-tipped Kneading Paddles of Co-rotating Twin Screw Extruders," *Society of Plastics Engineers ANTEC Technical Papers, 38* (1992) 1323-1327.

35. A. Lawal and D. M. Kalyon, "A Non-isothermal Model of Single Screw Extrusion Processing of Viscoplastic Materials Subject to Wall Slip," *Society of Plastics Engineers ANTEC Technical Papers, 38* (1992) 2158-2161.

36. A. Lawal and D. M. Kalyon, "Incorporation of Wall Slip in Non-isothermal Modeling of Single Screw Extrusion Processing," *Proceedings of the First International Conference on Transport Phenomena in Processing,* S. Guceri, ed., Technomic Publ. Co. (1992) 985-996.

37. A. Lawal, Z. Ji and D. M. Kalyon, "Computational Study of Chaotic Mixing in Co-Rotating Two-Tipped Kneading Paddles: Two-Dimensional Approach," *Polymer Engineering and Science,* 33, (3), (1992) 140-148.

38. D. M. Kalyon, "Simulation of Contiuous Processing of Highly Filled Suspensions," *Proceedings of Joint Ordnance Commanders Group, 6th Annual Meeting of the Continuous Extruder and Mixer Users Group,* sponsored by US Army and Navy, Phoenix, AZ, Nov., 1992.

39. A. Lawal and D. M. Kalyon, "Three Dimensional Analysis of Co-rotating Twin Screw Extrusion Using Tools of Dynamics," *Society of Plastics Engineers ANTEC Technical Papers, 39* (1993) 3397-3400.

40. A. Lawal and D. M. Kalyon, "Extrusion of Viscoplastic Fluids Subject to Different Slip Coefficients at Screw and Barrel Surfaces," *Society of Plastics Engineers ANTEC Technical Papers, 39* (1993) 2782-2785.

41. D. M. Kalyon, "Review of Factors Affecting the Continuous Processing and Manufacturability of Highly Filled Suspensions," *Journal of Materials Processing and Manufacturing Science, 2* (1993), 159-187.

42. A. Lawal, D. M. Kalyon and U. Yilmazer, "Extrusion and Lubrication Flows of Viscoplastic Fluids with Wall Slip," *Chem. Eng. Comm., 122* (1993) 127.

43. Y. Chen, D. M. Kalyon and E. Bayramli, "Effects of Surface Roughness and the Chemical Structure of Materials of Construction on Wall Slip Behavior of Linear Low Density Polyethylene in Capillary Flow," *J. Appl. Polym. Sci., 50* (7), (1993) 1169-1177.

44. A. Lawal and D. M. Kalyon, "A Non-isothermal Model of Single Screw Extrusion of Generalized Newtonian Fluids," *Numerical Heat Transfer, 26* (1), (1994) 103-121.

45. A. Lawal and D. M. Kalyon, "Single Screw Extrusion of Viscoplastic Fluids Subject to Different Slip Coefficients at Screw and Barrel Surfaces," *Polym. Eng. Sci., 34* (1994) 1471-1479.

46. A. Lawal and D. M. Kalyon, "Mechanisms of Mixing in Single Screw and Co-rotating Twin Screw Extruders," accepted to appear in *Polym. Eng. Sci.,* 1993.

47. A. Lawal and D. M. Kalyon, "Simulation of the Intensity of Segregation Distributions Using Three-Dimensional FEM Analyses: Applications to Co-rotating Twin Screw Extruders, submitted to *Journal of Applied Polymer Science,* 1994.

48. B. Aral and D. M. Kalyon, "Rheology and Extrudability of Very Concentrated Suspensions: Effects of Vacuum Imposition," submitted to *Plast. and Rubber Comp. Proc. and Applications,* 1994.

49. D. M. Kalyon, H. Gokturk, P. Yaras and B. Aral, "Motion Analysis of Development of Wall Slip During Die Flow of Concentrated Suspensions," submitted to *SPE ANTEC Technical Papers,* November 1994.

50. D. M. Kalyon, "Highly Filled Materials: Understanding the Generic Behavior of Highly Filled Materials Leads to Manufacturing Gains and New Technologies," accepted for publication in *ChemTech,* Feb. 1995.

51. D. M. Kalyon, "A Report on Highly Filled Materials and the Activities of the Highly Filled Materials Institute at SIT," submitted to *British Society Bulletin,* Feb. 1995.

C. MICROSTRUCTURAL ANALYSES OF HIGHLY FILLED MATERIALS

52. J. W. Sinton, J. C. Crowley, G. A. Lo, D. M. Kalyon and C. Jacob, "Nuclear Magnetic Resonance Imaging Studies of Mixing in Twin Screw Extruders," *Society of Plastics Engineers, ANTEC Technical Papers, 36* (1990) 116-119.

53. R. Yazici and D. M. Kalyon, "Characterization of Degree of Mixing of Concentrated Suspensions," *Society of Plastics Engineers ANTEC Technical Papers, 39* (1993) 2845-2850.

54. D. M. Kalyon, R. Yazici and A. Lawal, "Techniques to Analyze Goodness of Mixing of Concentrated Suspensions and Simulation of Mixing in Extrusion Flows," *Proceedings of 1993 JANNAF Propellant Development and Characterization Subcommittee Meeting,* Livermore, CA, April 28, 1993.

55. R. Yazici and D. M. Kalyon, "Degree of Mixing Analyses of Concentrated Suspensions by Electron Probe and X-Ray Diffraction," *Rubber Chem. and Techn., 66* (4), (1993) 527-537.

56. R. Yazici and D. M. Kalyon, "Analysis of Degree of Mixing in Extruded Profiles by Wide-Angle X-Ray Diffraction," submitted to *SPE ANTEC Technical Papers,* November 1994.

57. R. Yazici and D. M. Kalyon, "Quantitative Characterization of Degree of Mixedness of LOVA Grains," accepted for publication in *Journal of Energetic Materials,* March 1995.

D. POWDER CHARACTERIZATION

58. T. Fiske, S. Railkar and D. M. Kalyon, "Effects of Segregation on the Packing of Spherical and Non-Sypherical Particles," *Powder Technology, 81* (1994) 57-64.